Molecular Neurobiology (2019) 56:1719–1736
https://doi.org/10.1007/s12035-018-1186-6

Requirement of the Mowat-Wilson Syndrome Gene *Zeb2* in the Differentiation and Maintenance of Non-photoreceptor Cell Types During Retinal Development

Wen Wei[1] · Bin Liu[1,2] · Haisong Jiang[3] · Kangxin Jin[1] · Mengqing Xiang[1,3,4]

Received: 4 April 2018 / Accepted: 7 June 2018 / Published online: 19 June 2018

Abstract

Mutations in the human transcription factor gene *ZEB2* cause Mowat-Wilson syndrome, a congenital disorder characterized by multiple and variable anomalies including microcephaly, Hirschsprung disease, intellectual disability, epilepsy, microphthalmia, retinal coloboma, and/or optic nerve hypoplasia. *Zeb2* in mice is involved in patterning neural and lens epithelia, neural tube closure, as well as in the specification, differentiation and migration of neural crest cells and cortical neurons. At present, it is still unclear how *Zeb2* mutations cause retinal coloboma, whether *Zeb2* inactivation results in retinal degeneration, and whether Zeb2 is sufficient to promote the differentiation of different retinal cell types. Here, we show that during mouse retinal development, Zeb2 is expressed transiently in early retinal progenitors and in all non-photoreceptor cell types including bipolar, amacrine, horizontal, ganglion, and Müller glial cells. Its retina-specific ablation causes severe loss of all non-photoreceptor cell types, cell fate switch to photoreceptors by retinal progenitors, and elevated apoptosis, which lead to age-dependent retinal degeneration, optic nerve hypoplasia, synaptic connection defects, and impaired ERG (electroretinogram) responses. Moreover, overexpression of Zeb2 is sufficient to promote the fate of all non-photoreceptor cell types at the expense of photoreceptors. Together, our data not only suggest that Zeb2 is both necessary and sufficient for the differentiation of non-photoreceptor cell types while simultaneously inhibiting the photoreceptor cell fate by repressing transcription factor genes involved in photoreceptor specification and differentiation, but also reveal a necessity of Zeb2 in the long-term maintenance of retinal cell types. This work helps to decipher the etiology of retinal atrophy associated with Mowat-Wilson syndrome and hence will impact on clinical diagnosis and management of the patients suffering from this syndrome.

Keywords Zeb2 · Transcription factor · Mowat-Wilson syndrome · Retinal development · Retinal ganglion cell · Photoreceptor

Electronic supplementary material The online version of this article (https://doi.org/10.1007/s12035-018-1186-6) contains supplementary material, which is available to authorized users.

✉ Kangxin Jin
kxjin@yahoo.com

✉ Mengqing Xiang
xiang@cabm.rutgers.edu; xiangmq3@mail.sysu.edu.cn

[1] State Key Laboratory of Ophthalmology, Guangdong Provincial Key Laboratory of Ophthalmology and Visual Science, Zhongshan Ophthalmic Center, Sun Yat-sen University, Guangzhou 510060, China

[2] Present address: Institute for Metabolic and Neuropsychiatric Disorders, Binzhou Medical University Hospital, Binzhou, China

[3] Center for Advanced Biotechnology and Medicine and Department of Pediatrics, Rutgers University-Robert Wood Johnson Medical School, 679 Hoes Lane West, Piscataway, NJ 08854, USA

[4] Guangdong Provincial Key Laboratory of Brain Function and Disease, Zhongshan School of Medicine, Sun Yat-sen University, Guangzhou 510080, China

Introduction

The mammalian retina is a multilayered sensorineural epithelium composed of seven major types of neurons and glial cells that include the rod, cone, bipolar, horizontal, amacrine, ganglion, and Müller cells. The generation of proper types and quantities of these cells during development is essential to establish a fully functional retina, and their long-term maintenance in the adult is necessary to sustain normal vision. Retinal cell development and maintenance are exquisite processes that require coordinated regulatory actions by various intrinsic and extrinsic factors [1–8]. Perturbation of any of these regulatory mechanisms may lead to aberrant retinal development, retinal dysfunction, and various degenerative retinal diseases such as microphthalmia, retinitis pigmentosa, cone-rod dystrophy and Leber congenital amaurosis [9, 10].

Zeb2 (zinc finger E-box binding homeobox 2), also known as Sip1 (Smad-interacting protein 1) and Zfhx1b, is a member

of the family of two-handed zinc-finger/homeodomain transcription factors [11–13]. A number of mutations in the human *ZEB2* gene are reported to cause the congenital Mowat-Wilson syndrome (MWS, MIM#235730), which is characterized by a set of distinct facial features in association with variable anomalies including microcephaly, agenesis of corpus callosum, Hirschsprung disease or intestinal aganglionosis, heart defect, urogenital malformation, strabismus, intellectual disability, and epilepsy [14–19]. In addition, structural ocular phenotypes are often associated with Mowat-Wilson syndrome but significantly under-recognized. Patients may present microphthalmia, chorioretinal and iris coloboma, optic nerve hypoplasia, cataract, and/or high myopia [15, 17, 18, 20–25]. Independent of Mowat-Wilson syndrome, a genome-wide association study, has also identified *ZEB2* as a susceptibility locus for severe myopia [26]. The function of Zeb2 during development has been studied in mice by conventional and conditional gene targeting. These analyses have shown that *Zeb2* ablation results in a wide range of phenotypes such as mis-specification and defective migration of cortical neurons, craniofacial malformations, severe intestinal aganglionosis, heart defect, and abnormal lens and retinal development, which resemble those of patients with Mowat-Wilson syndrome [27–33]. However, it is still unclear how *Zeb2* mutations cause retinal coloboma, whether *Zeb2* inactivation results in retinal degeneration, and whether Zeb2 as a transcription factor is sufficient to promote the differentiation of different retinal cell types.

We have previously established a Foxn4-Ptf1a-Tfap2a/2b transcription factor pathway essential for the determination and differentiation of amacrine and horizontal cells during retinal development [34–36]. However, this regulatory pathway is still far from complete and additional components are yet to be defined. For instance, Pft1a has a strong activity to promote the differentiation of amacrine cells including the dopaminergic subtype, whereas Tfap2a or 2b displays a much weaker activity in promoting amacrine cell differentiation and is unable to promote the differentiation of dopaminergic amacrine cells [36]. Similarly, Prdm13 has been shown to act downstream of Ptf1a to regulate amacrine cell development, but unlike Ptf1a, is not required for subtype specification of dopaminergic or cholinergic amacrine cells [37]. Thus, there are likely additional regulatory factors involved in the Foxn4-Ptf1a-Tfap2a/2b transcription factor pathway to control amacrine and horizontal cell development during retinogenesis. Here, we identify Zeb2 as a downstream transcriptional regulator of this pathway and demonstrate that Zeb2 is both necessary and sufficient for the differentiation and survival of non-photoreceptor cell types. Moreover, conditional *Zeb2* inactivation may lead to a cell fate switch in retinal progenitors to photoreceptors from non-photoreceptor cell types.

Materials and Methods

Mice

All procedures in animals were performed according to the IACUC standards, and approved by Zhongshan Ophthalmic Center, Sun Yat-sen University and Rutgers University. The conditional $Zeb2^{\Delta fl/\Delta fl}$ knock-out mice were generated by mating between Six3-Cre and $Zeb2^{fl/fl}$ animals and maintained by breeding with C57BL6/J mice. A floxed *Zeb2* mouse line [38] was bred with the Six3-Cre transgenic line [39] to delete exon 7 of *Zeb2* in the developing retina to obtain the $Zeb2^{\Delta fl/\Delta fl}$ (Six3-Cre;$Zeb2^{fl/fl}$) and control ($Zeb2^{+/+}$, $Zeb2^{+/fl}$, $Zeb2^{fl/fl}$ or Six3-Cre;$Zeb2^{+/+}$) mice. The C57BL6/J mice were purchased from the Vital River Laboratories (Beijing), and the CD1 mice from the Charles River Laboratories (Wilmington, MA). The starting stage of mouse embryos was defined by taking the morning as E0.5 when the copulation plug was seen. All genotypes were determined by PCR.

Microarray and RNA-Seq Analyses

Microarray profiling was performed as previously described [40] using probes derived from retinal RNA of E14.5 $Ptf1a^{Cre/Cre}$ [34, 41] and $Ptf1a^{+/+}$ embryos. The GeneChip mouse expression arrays (430A; Affymetrix) were hybridized and scanned, and the signal intensity and detection (absence/presence) calls were determined using the Microarray Suite software (Affymetrix). Upregulated and downregulated genes with statistical significance were identified by the DNA-Chip Analyzer (dChip) software package [42]. The R software was used to draw the heatmap and scatter and volcano plots of gene expression levels.

RNA-Seq was carried out as described previously [36]. Total RNA was extracted from P0 control and $Zeb2^{\Delta fl/\Delta fl}$ retinas using the TRIzol reagent (Invitrogen) according to the manufacturer's instruction. Ribosomal RNA was depleted prior to RNA-seq library preparation. The obtained sequence reads were trimmed and mapped to the mouse reference genome (mm10) using Tophat, and gene expression and changes were analyzed using Cufflinks. Scatter and volcano plot analyses of gene expression levels were performed using the R software. Gene set enrichment analysis (GSEA) was carried out as described [43], which was followed by network visualization in Cytoscape using the EnrichmentMap plugin [44, 45].

RNA In Situ Hybridization

RNA in situ hybridization was carried out as described previously [46]. Digoxigenin-labeled riboprobes were prepared following the manufacturer's protocol (Roche Diagnostics). To prepare the hybridization probe, brain tissues from P14 wild-type mice were dissected out, and total RNA was extracted

from the tissue using TRIzol, which was subsequently converted to cDNA using the PrimeScript 1st Strand cDNA Synthesis Kit (Takara). *Zeb2* DNA fragment was amplified by PCR from the cDNA with the primers 5'-GTGGATCCCATGCG AACTGCCATCTG and 5′-TCGAATTCTATGCCTCTCGA GCTGGG, and subcloned into the pBluescript vector.

Antibodies and Immunostaining

Tissue processing and immunostaining were carried out as described previously [35, 47]. The following primary antibodies were used: mouse anti-Brn3a (1:500, Cat: MAB1585, Millipore); goat anti-Brn3b (1:500, Cat:sc-6026, Santa Cruz Biotech.); goat anti-Bhlhb5/BETA3 (1:2000, Cat: sc-6045, Santa Cruz Biotech.); rabbit anti-calbindin D-28 k (1:3000, Cat: CB-38, Swant); goat anti-Chx10 (1:2000, Cat: sc-21690, Santa Cruz Biotech.); rabbit anti-GABA (1:1000, Cat: a2052, Sigma); mouse anti-GAD65 (1:500, Cat: 559931, BD Biosciences); mouse anti-GAD67 (1:500, Cat: MAB5406, Millipore); rabbit anti-GFP (1:1000, Cat: 598, MBL International); goat anti-GFP (1:2000, Cat: ab6673, Abcam); chicken anti-GFP (1:2000, Cat: ab13970, Abcam); mouse anti-glutamine synthetase (1:1000, Cat: mab302, Millipore); goat anti-GLYT1 (1:2000, Cat: AB1770, Millipore); mouse anti-Lim1/2 [1:10, Cat: 4F2, Developmental Studies Hybridoma Bank (DSHB)]; rabbit anti-Pax6 (1:2000, Cat: ab2237, Millipore); mouse anti-Pax6 (1:1000, Cat: pax6, DSHB); rabbit anti-recoverin (1:4000, Cat: ab5585, Millipore); Mouse anti-syntaxin (1:1000, Cat: S0664, Sigma); rabbit anti-Sox9 (1:8000, Cat: ab5535, Millipore); rabbit anti-Tfap2a/2b (1:1000, Cat: ab11828, Abcam); mouse anti-rhodopsin (1:20, 1D4 [48]); rabbit anti-GFAP (1:1000, Cat: Z0334, DAKO); rabbit anti-protein kinase Cα (1:15000, Cat: P4334, Sigma); rabbit anti-Ki67 (1:100, Cat: MA5–14520, Thermo Fisher); goat anti-Sox2 (1:100, Cat: sc-17320, Santa Cruz Biotech.); mouse anti-Isl1 (1:500, Cat: 40.2D6-s, DSHB); rabbit anti-ZEB2(H-260)(1:100, Cat: sc-48789, Santa Cruz Biotech.); rabbit anti-active Caspase-3 (1:100, Cat: 559565, BD Biosciences); mouse anti-PNR (NR2E3) (1:500, Cat: pp-h7223–000, Persesus Proteomics); rabbit anti-tyrosine hydroxylase (1:1000, Cat: ab152, Millipore); mouse anti-synaptophysin (1:500, Cat: S5768, Sigma); rabbit anti-RXRγ (Rxrg) (1:500, Cat: sc-555, Santa Cruz Biotech.); mouse anti-Ctbp2 (Ribeye) (1:1000, Cat: 612044, BD Biosciences). Secondary antibodies conjugated with Alexa Fluor 488 or 594 were used (Life Technologies). Images were captured by the LSM700 confocal system (Zeiss).

Electroretinogram (ERG) and Optic Coherence Tomography (OCT)

To assess retinal function, ERG responses were recorded in 5 $Zeb2^{\Delta fl/\Delta fl}$ and 5 control 1-month-old littermates, and in 3 $Zeb2^{\Delta fl/\Delta fl}$ and 3 control 6-month-old littermates. All animals were recorded under the same settings and conditions.

Mice were dark-adapted overnight before ERG recordings. Under weak red light, mice were anesthetized with intraperitoneal injection of chloral hydrate (4.5 μg/g body weight) [49]. Pupils were dilated by tropicamide phenylephrine eye drops, and eyes were kept moist with a drop of hypromellose. Gold wire loops were positioned on the surface of cornea as the active electrode. Needle electrodes were inserted into the skin of temporal canthus and the base of tail respectively as reference and ground leads. Impedance of all electrodes maintained at < 5 kΩ. ERG data were recorded using the RETI-scan system (Roland Consult, RETI-scan, Germany) at a sampling rate of 2 kHz. During the experiments, mice were placed on a heated platform with a circulating water pump bath to maintain a constant 37 °C temperature [49, 50].

During ERG recording, mice were tested under dark adaptation first. They were exposed to full-field scotopic flashes of 1.3 ms duration presented by a Ganzfeld (Roland Consult, Germany) with different intensities: 0.003, 0.01, 0.03, 0.1, 0.3, 1.0, 3.0, 10 cd.s/m^2. Flash stimuli above 10 cd.s/m2 were delivered by a Xenon lamp, and those below 10 cd.s/m^2 were delivered by a green (525 nm) LED [14]. Mice were light-adapted with a saturating background (green, 20 cd.s/m^2) for 5 min, five levels of stimuli were used for the photopic recordings (0.3, 1.0, 3.0, 10, 30 cd.s/m^2).

Data analysis was performed using the RETI port software (Roland) following 50 Hz low-pass filtering [49]. The a-wave amplitude was measured from baseline to first negative peak, and b-wave amplitude was measured from a-wave trough to the next positive peak.

For OCT, imaging was conducted in 4 $Zeb2^{\Delta fl/\Delta fl}$ and 3 control 1-month-old littermates. Mice were anesthetized with intraperitoneal injection of chloral hydrate (4.5 μg/g body weight). Pupils were dilated by tropicamide phenylephrine eye drops, and eyes were kept moist with a drop of hypromellose. One eye was randomly selected for the optic nerve head scan. OCT images were captured using the Spectralis OCT (Heidelberg, Germany) with a 30° field. A 30D standard ophthalmic non-contact slit lamp lens (Volk Optical Inc., Ohio, USA) was positioned in front of the Heidelberg Spectralis optic. Volume scans centered on the optic nerve head were acquired in the automatic real-time mode (ART), averaging 50 frames per image.

Real-Time Quantitative Reverse Transcription (qRT)-PCR

Retinas of P0 control and $Zeb2^{\Delta fl/\Delta fl}$ mice were dissected out the eyeball and harvested. Total RNA was isolated using the TRIzol reagent (Invitrogen). RNA (1 μg) from each sample of different genotypes was converted to cDNA using the HiScript II Q RT SuperMix for qPCR (Vazyme Biotech).

qRT-PCR was performed using the Kapa SYBR fast qPCR master mix (Kapa) and Light Cycler® 384 Real-Time PCR system (Roche). Relative quantities were calculated by the comparative cycle threshold method (ΔΔCT method) [51]. All data were tested for significance using two-sample Student's *t* test. The primer sequences used for qRT-PCR were described [52, 53] and listed in Table S1.

Plasmid Construction and Electroporation

The pCIG vector was reported previously [54, 55], which contains the CAG promotor/enhancer, multiple cloning sites (MCS), IRES-eGFP, and rabbit β-globin PolyA sequences. The plasmid containing the *Zeb2* ORF was purchased from GeneCopeia. To construct the pCIG-Zeb2 plasmid, the ORF of *Zeb2* was subcloned into the MCS of the pCIG vector.

For in vivo electroporation, P0 CD1 mouse pups were anesthetized by chilling on ice. 1 μl of pCIG-GFP (3 μg/μl) or pCIG-Zeb2 (3 μg/μl) DNA solution plus 0.1% Fast Green dye was injected into the subretinal space using a Microliter Syringe (Hamilton). Immediately following injection, electric pulses (100 V; five 50-ms pulses with 950-ms intervals) were applied with tweezer-type electrodes using the pulse generator ECM 830 (BTX). Transfected retinas were collected at P12 for analysis as described previously [36, 55].

For ex vivo electroporation and retinal cup culture, E14.5 embryos of CD1 mice were removed from anesthetized mothers by caesarian section. After all embryos were removed, the anesthetized mother was sacrificed. 1 μl of DNA solution of pCIG-GFP (3 μg/μl) or pCIG-Zeb2 (3 μg/μl) plus 0.1% Fast Green dye was injected into the subretinal space of E14.5 embryos using a Microliter Syringe (Hamilton). The "+" electrode of tweezer-type electrodes (BTX) was positioned on the injected eye, and the "-" electrode on the opposite eye. Five 50-ms electric pulses were then delivered at 40 V with 950 ms intervals as described [56, 57]. After ex vivo electroporation, the eyeball was removed and retinal cup was prepared and cultured in explant culture medium [58] at 37 °C for 4.5 days. Then the electroporated retinal cups were harvested and fixed for 20 min with 4% paraformaldehyde for further analysis.

Quantification and Statistical Analysis

For conditional ablation experiments, at least three retinas were analyzed for each control and $Zeb2^{\Delta fl/\Delta fl}$ animals. For each retina, cell marker counting was obtained from 5 to 12 non-overlapping fields in similar retinal regions. Each field was photographed using the confocal microscope at 400 x magnification. For misexpression experiments, depending on the frequency or ratio of each cell type, hundreds to thousands of GFP^+ cells in each transfected retina were scored. And at least 3 retinas were counted for each individual cell marker. The retinas were transfected with the pCIG-GFP or pCIG-Zeb2 plasmid.

Statistical analysis was performed using the GraphPad Prism 6.0 and Microsoft Excel computer programs. The results are expressed as mean ± SD for experiments conducted at least in triplicates. Unpaired two-tailed Student's *t* test was used to assess differences between two groups, and a value of $p < 0.05$ was considered statistically significant.

Results

Downregulation of *Zeb2* Expression in the *Ptf1a* Mutant Mouse Retina

To identify additional component in the Foxn4-Ptf1a-Tfap2 transcription factor pathway that controls the development of retinal amacrine and horizontal cells, we performed an Affymetrix microarray analysis using probes derived from E14.5 $Ptf1a^{+/+}$ and $Ptf1a^{Cre/Cre}$ retinas [34, 41]. The obtained data were analyzed using the Affymetrix Microarray Suite software to obtain absence/presence calls and the dChip software package to calculate fold changes of transcripts between the control and mutant retinas [40, 42]. Further bioinformatic analysis uncovered a large set of downregulated transcripts and a smaller set of upregulated transcripts in the mutant retina (Fig. 1a–c; Table S2). Among the 482 transcripts whose expression was significantly altered (change ≥ 1.5-fold, $p < 0.05$) in *Ptf1a* null mutant retinas, we found that *Tfap2a* and *Tfap2b* were among the most downregulated transcripts (Table S2), consistent with our previous report [36]. In addition, we noticed that the expression of the *Zeb2* gene was downregulated by approximately two-fold (Fig. 1d), suggesting that *Zeb2* may be expressed in amacrine and horizontal cells and play a role in regulating their development.

Pattern of *Zeb2* Expression during Mouse Retinal Development

To confirm the expression of *Zeb2* in amacrine and horizontal cells, we investigated its spatial and temporal expression pattern during mouse retinal development by RNA in situ hybridization and immunofluorescent staining. At E12.5, there was weaker *Zeb2* RNA signal in the central retina and stronger *Zeb2* signal in the lens (Fig. 2a). From E14.5 to E18.5, strong signal appeared in the entire retina within both the outer and inner neuroblastic layers (Fig. 2b–d). At early postnatal stages, *Zeb2* signal gradually disappeared from the outer neuroblastic layer and was limited to inner layers of the retina (Fig. 2e, f). From P12 and beyond, it was essentially restricted only to the inner nuclear layer (INL) and ganglion cell layer (GCL) (Fig. 2g, h). Consistent with the profile of the RNA in situ hybridization signal, RNA-seq analysis of developmental

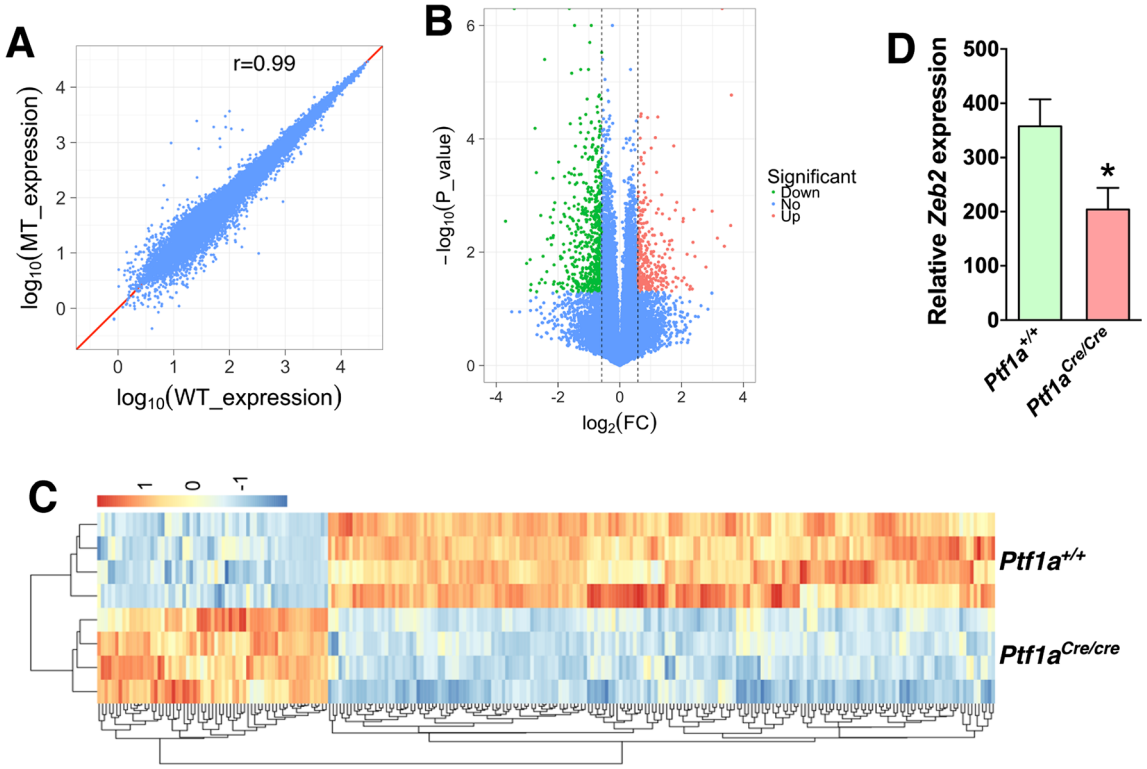

Fig. 1 Expression array analysis of differentially expressed genes in E14.5 *Ptf1a*$^{Cre/Cre}$ retinas. **a** Scatter plot of probe hybridization signals. Transcript expression levels are depicted in $\log_{10}$ scale. The diagonal line represents equal expression in the two genotypes (WT, wild type; MT, mutant). The Pearson correlation coefficient is indicated. **b** Volcano plot (significance vs fold change) of significantly downregulated (green) and upregulated (red) genes (fold change ≥ 1.5 and $p < 0.05$) between the wild type and mutant retinas. **c** Cluster analysis reveals a large group of significantly downregulated genes and a smaller group of significantly upregulated genes in the mutant retina. **d** Decreased expression of *Zeb2* in the *Ptf1a*$^{Cre/Cre}$ retina. Data are presented as mean ± SD ($n = 4$). *$p <$ 0.005

stage-specific retinal transcriptomes (KJ and MX, unpublished) showed that *Zeb2* had a high level of expression from E13.5 to P6, which was reduced by approximately 2-fold from P6 to P13, and then kept at this low level up to at least 9 months (Fig. 2i).

The Zeb2 protein has a very similar expression pattern as its RNA transcripts. From E12.5 to E14.5, its expression spread from the central retina to the entire retina in most progenitor cells while remaining strong in lens cells (Fig. 2j–l). At E18.5, it was distributed in most cells of the outer and inner neuroblastic layers but absent from most cells at the outer edge of the retina where photoreceptor precursors and newborn photoreceptors reside (Fig. 2m), suggesting that Zeb2 may be expressed in most retinal progenitor cells at this stage. Consistent with this idea, Zeb2 was extensively colocalized with Ki67 in dividing progenitors (Fig. 2r, s). From P0 to P8, Zeb2 was gradually downregulated from progenitors and limited to the INL and GCL although migrating Zeb2-positive horizontal cells were still visible within the outer nuclear layer (ONL) (Fig. 2n–p). In P12 and mature retinas, numerous Zeb2-immunoreactive cells remained in the INL and GCL (Fig. 2q). Therefore, Zeb2 is transiently expressed in progenitors and then permanently expressed in most cells of the inner retina as retinal development progresses.

Located in the INL and GCL are ganglion cells, Müller cells and three types of interneurons including bipolar, amacrine and horizontal cells. To determine which of these cell types express Zeb2, we carried out double-immunofluorescent labeling of P21 mouse retinal sections using antibodies against Zeb2 and several cell type- and subtype-specific markers. We found coexpression of Zeb2 in 52.5% Chx10- and 36.2% Isl1-immunoreactive bipolar cells, in 14.4% PKCα^+ (protein kinase α) rod bipolar cells, and in 32.7% Bhlhb5$^+$ type 2 OFF-cone bipolar cells (Fig. 3a–d, m). There was an extensive colocalization between Zeb2 and Pax6, a TF marker for amacrine, horizontal and ganglion cells (Fig. 3e, m). Consistent with this, Zeb2 was coexpressed in approximately 80% GAD65$^+$ and GAD67$^+$ GABAergic amacrine cells, in 78.4% GLYT1$^+$ glycinergic amacrine cells, in 100% calbindin$^+$ horizontal cells, and in 70% Brn3a$^+$ ganglion cells (Fig. 3f–j, m). Furthermore, Zeb2 was seen in 81.0% Sox2$^+$ and 84.3% GS$^+$ (glutamine synthetase) Müller cells (Fig. 3k–m). The lack of labeling in the outer nuclear layer indicated the absence of Zeb2 expression in rod and cone cells. These results together thus demonstrate the expression of Zeb2 in most or all amacrine, horizontal, ganglion and Müller cells, in a smaller subpopulation of rod and cone bipolar cells, but not in photoreceptors. In a previous report, Zeb2

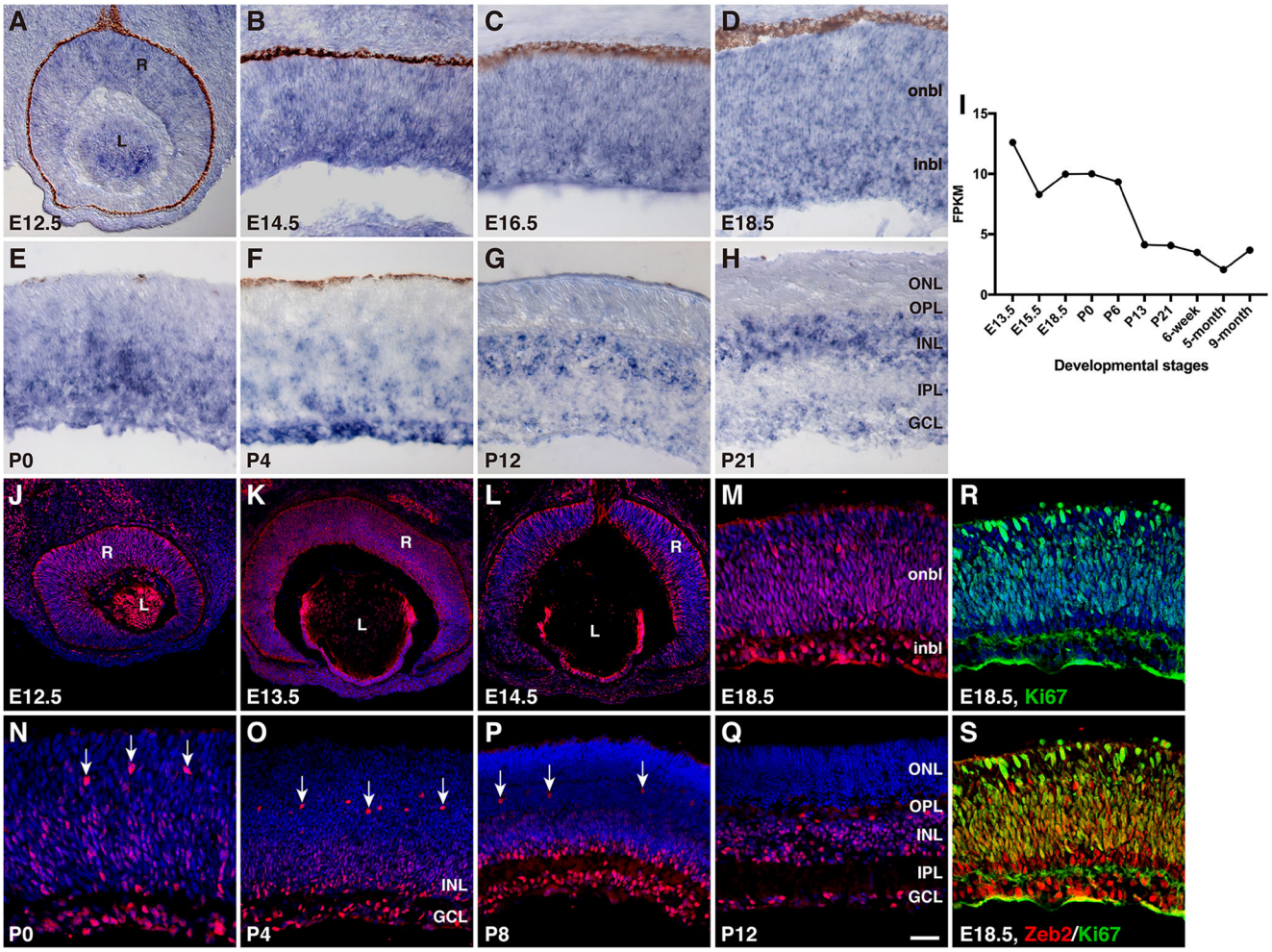

Fig. 2 Spatiotemporal expression pattern of *Zeb2* during mouse retinal development. **a–h** Retinal sections from the indicated developmental stages were in situ hybridized with a *Zeb2* probe. **i** Temporal expression levels (FPKM) of *Zeb2* from embryonic to adult stages during retinal development as determined by RNA-seq analysis. **j–q** Retinal sections from the indicated developmental stages were immunostained with an anti-zeb2 antibody and counterstained with DAPI. Arrows point to migrating horizontal cells. **r**, **s** The section in (M) was co-labeled with an anti-Ki67 antibody. Abbreviations: GCL, ganglion cell layer; inbl, inner neuroblastic layer; INL, inner nuclear layer; IPL, inner plexiform layer; L, lens; onbl, outer neuroblastic layer; ONL, outer nuclear layer; OPL, outer plexiform layer; R, retina. Scale bar: **a**, **p**, 40 μm; **b–h**, **n**, 20 μm; **j**, 66.7 μm; **k**, **l**, 80 μm; **m**, **r**, **s**, 25 μm; **o**, **q**, 33.3 μm

was shown not to be expressed in bipolar and Müller cells of the P14 mouse retina [33]. To verify this observation, we investigated the cell-type distribution of Zeb2 protein in the P12 mouse retina. The result was similar to that of P21 retina except that Zeb2 was present only in 2.1% PKCα^{+} rod bipolar cells at P12 (Fig. 3a′–m′). Therefore, at earlier postnatal stages, Zeb2 has already been distributed to most Müller cells, a subset of cone bipolar cells, and a very small subpopulation of rod bipolar cells.

Conditional Ablation of *Zeb2* Causes Retinal Developmental Defects and Degeneration

To understand how *Zeb2* mutations may lead to retinal coloboma associated with Mowat-Wilson syndrome, we conditionally inactivated *Zeb2* in retinal progenitor cells using a floxed *Zeb2* allele and the Six3-Cre driver mouse line [38, 39] (Fig. 4a). Previously, Cre-mediated deletion of exon 7 of *Zeb2* was shown to result in a null allele [38]. Consistent with this, Zeb2 protein expression was near completely eliminated in $Zeb2^{\Delta fl/\Delta fl}$ (Six3-Cre;$Zeb2^{fl/fl}$) retinas (Fig. 4u, v).

At a gross level, there is obvious size reduction of the optic nerve, optic tract and optic chiasm in $Zeb2^{\Delta fl/\Delta fl}$ mice compared to the control (Fig. 4c–e). OCT (optic coherence tomography) showed that $Zeb2^{\Delta fl/\Delta fl}$ animals had much thinned retinas with a swelled optic disc (Fig. 4b). Consistent with these observations, hematoxylin-eosin (HE) and DAPI staining of retinal sections from P0 to 6-month mice revealed a progressive degeneration of the mutant retina (Fig. 4f–n, s–z). The retinas of the control and $Zeb2^{\Delta fl/\Delta fl}$ mice are only slight different in thickness at P0 and P7 (Fig. 4f–i, n, s, t). At P12, P14 and P21, the mutant retina has a typical laminar organization

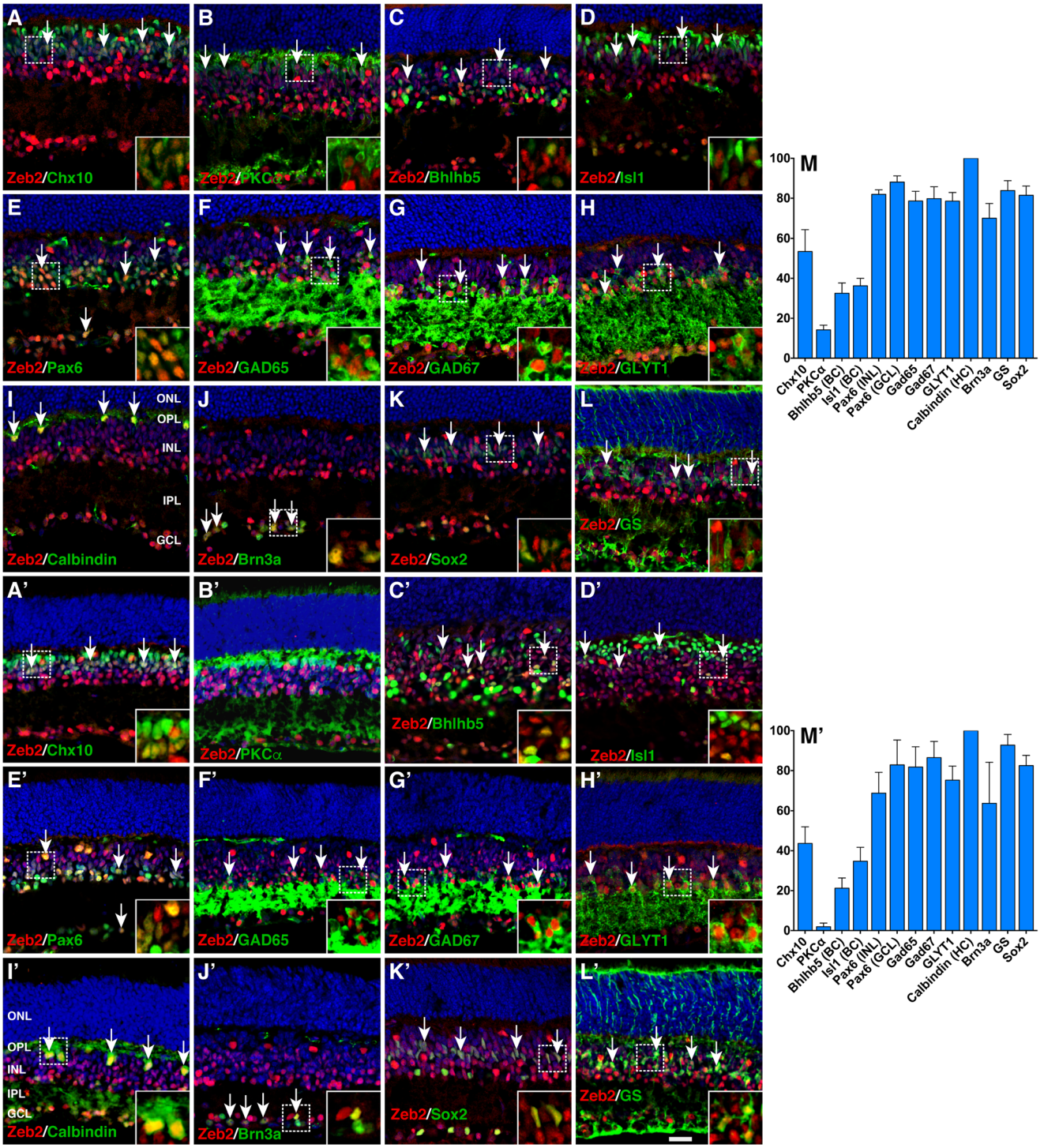

Fig. 3 Retinal cell types in which Zeb2 is expressed. **a–l** Sections from P21 mouse retinas were double-immunolabeled with an anti-Zeb2 antibody and those against the indicated cell type-specific protein markers. Blue indicates nuclear DAPI counterstaining. Arrows point to representative colocalized cells and insets show corresponding outlined regions at a higher magnification. **m** Percentages of marker-positive retinal cells that are immunoreactive for Zeb2 at P21. Data are presented as mean ± SD ($n = 3$). **a′–l′** Sections from P12 mouse retinas were double-immunolabeled with an anti-Zeb2 antibody and those against the indicated cell type-specific protein markers. Arrows point to representative colocalized cells and insets show corresponding outlined regions at a higher magnification. **m′** Percentages of marker-positive retinal cells that are immunoreactive for Zeb2 at P12. Data are presented as mean ± SD ($n = 3$). Abbreviations: BC, bipolar cell; GCL, ganglion cell layer; GS, glutamine synthetase; HC, horizontal cell; INL, inner nuclear layer; IPL, inner plexiform layer; ONL, outer nuclear layer; OPL, outer plexiform layer. Scale bar: **a–l**, **a′–l′**, 20 μm

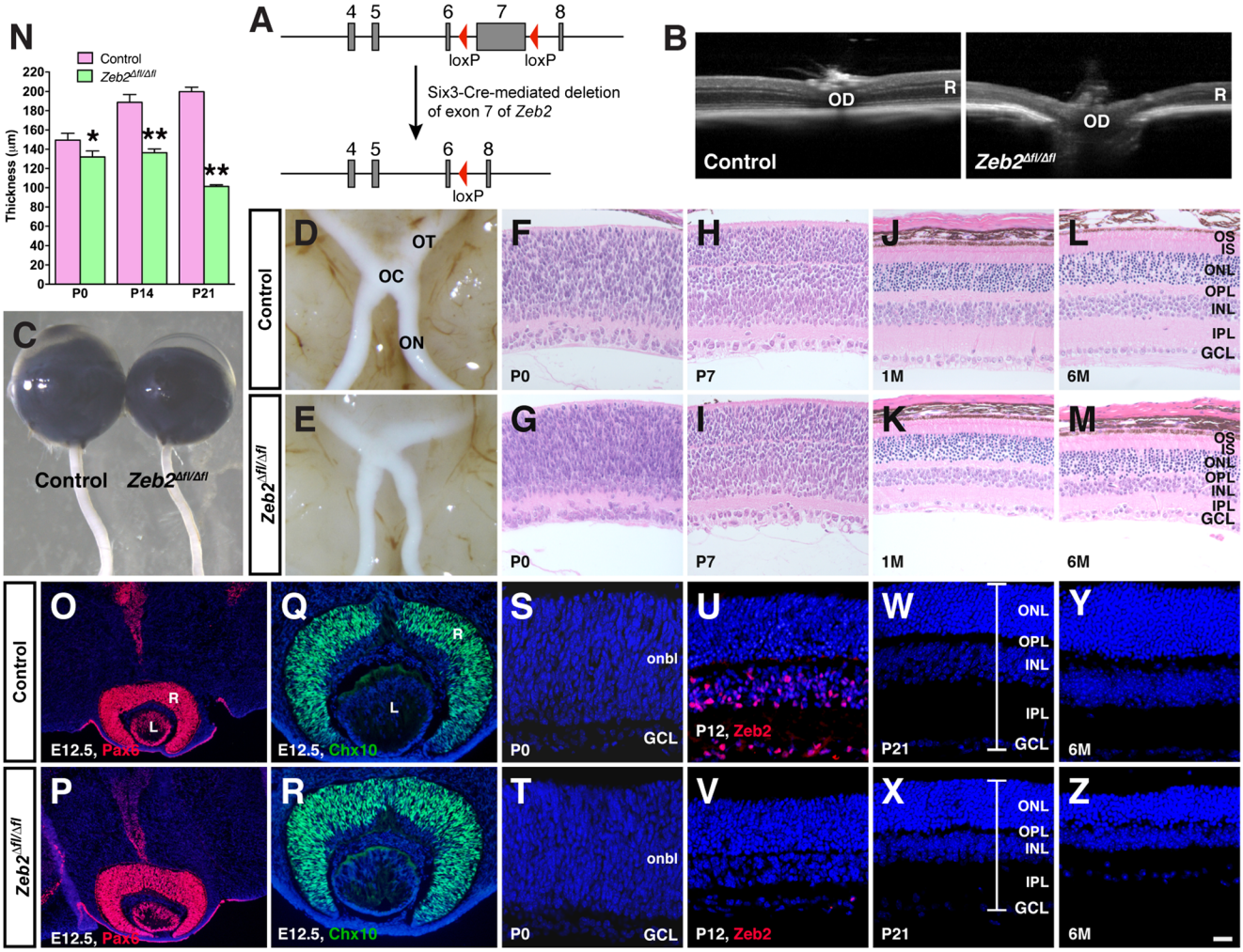

Fig. 4 Gross defects in *Zeb2*$^{\Delta fl/\Delta fl}$ retinas. **a** A floxed *Zeb2* mouse line was bred with the Six3-Cre transgenic line to conditionally delete exon 7 of *Zeb2* in the developing retina. **b** Thinned retina and swelled optic disc in 1-month-old *Zeb2*$^{\Delta fl/\Delta fl}$ mice as determined by OCT. **c** The optic nerve size is diminished in P21 *Zeb2*$^{\Delta fl/\Delta fl}$ animals. **d**, **e** The size of the optic nerve, optic tract, and optic chiasm is all decreased in P21 *Zeb2*$^{\Delta fl/\Delta fl}$ mice. **f–m** Laminar structures were visualized in P0, P7, 1-month (1 M), and 6-month (6 M) retinal sections by hematoxylin-eosin staining. Compared to the control, there is a progressive decrease in the thickness of the *Zeb2*$^{\Delta fl/\Delta fl}$ retina. **n** The retinal thickness of the control and *Zeb2*$^{\Delta fl/\Delta fl}$ retinas, visualized by nuclear DAPI labeling (as outlined in **w**, **x**), was quantified at P0, P14, and P21. Each histogram represents the mean ± SD for three retinas. $*p < 0.05$; $**p < 0.001$. **o–r** Immunostaining of E12.5 control and *Zeb2*$^{\Delta fl/\Delta fl}$ retinal sections with antibodies against Pax6 or Chx10. **s–z** P0, P12, P21, and 6-month retinal sections from control and *Zeb2*$^{\Delta fl/\Delta fl}$ animals were labeled with nuclear DAPI. P12 sections were also co-labeled with an anti-Zeb2 antibody to confirm *Zeb2* ablation in the *Zeb2*$^{\Delta fl/\Delta fl}$ retina (**u**, **v**). Abbreviations: GCL, ganglion cell layer; INL, inner nuclear layer; IPL, inner plexiform layer; IS, inner segment; L, lens; OC, optic chiasm; OD, optic disc; ON, optic nerve; ONL, outer nuclear layer; OPL, outer plexiform layer; OS, outer segment; OT, optic tract; R, retina. Scale bar: **o**, **p**, 100 μm; **q**, **r**, 50 μm; **f–m**, **s–z**, 25 μm

containing all the cellular layers; however, compared to the control, it is overtly decreased in thickness with the INL, IPL and GCL most affected (Fig. 4n, u–x). At 1 month of age, all layers of the mutant retina including the ONL and the inner and outer segments of photoreceptors appear to diminish in thickness (Fig. 4j, k). By 6 months, the mutant retina is further reduced in thickness. Compared to the control, in the *Zeb2*$^{\Delta fl/\Delta fl}$ retina, the ONL and INL cells sometimes intermingle and the OPL becomes obscure (Fig. 4l, m).

Zeb2 ablation does not appear to alter the number of Pax6-immunoreactive or Chx10-immunoreactive progenitors in E12.5 mutant retinas compared to the control (Fig. 4o-r). In addition, there are similar numbers of Ki67^{+} dividing progenitor cells in control and mutant retinas at P0 and P4 (Fig. S1 h-l), suggesting that Zeb2 may not be involved in retinal progenitor proliferation. By contrast, there is a significant increase of apoptotic cell death in *Zeb2*$^{\Delta fl/\Delta fl}$ retinas at P0, P4, P14 and P21 as determined by immunoreactivity of the activated caspase 3 (Fig. S1a-g). Given the expression of Zeb2 in non-photoreceptor cells, these results suggest that Zeb2 may play a key role in the specification, differentiation and/or survival of these cells. The later onset of photoreceptor loss

indicates that photoreceptors may be gradually degenerated due to primary loss of non-photoreceptor cells in the *Zeb2* mutant retina.

Loss of Non-photoreceptor Cells and Synaptic Defects in the *Zeb2* Mutant Retina

To determine whether there is differential loss of cell types in the $Zeb2^{\Delta fl/\Delta fl}$ retina, we investigated the cell types and subtypes present in the mutant retina by immunofluorescence using a battery of cell type-specific antibodies. In the P21 control retina, an anti-Pax6 antibody stained amacrine and ganglion cells in the INL and GCL. In the mutant, however, there was a great decrease in the abundance of Pax6-immunoreactive cells (Fig. 5a, a′). Consistent with this, there was a steep loss in the expression of general amacrine cell markers as well as subtype-specific amacrine cell markers in the mutant retina. These include general amacrine cell markers syntaxin and calbindin, GABAergic amacrine cell markers GAD65 and GABA, glycinergic amacrine cell marker GLYT1, and dopaminergic amacrine cell marker TH (tyrosine hydroxylase) (Fig. 5b–e, b′–e′; Fig. S2a, b, a', b'). Similarly, there was a dramatic loss of horizontal cells immunoreactive for calbindin and Lim1, and ganglion cells immunoreactive for Brn3a and Brn3b in $Zeb2^{\Delta fl/\Delta fl}$ retinas (Fig. 5e, h, i, e′, h′, i′; Fig. S2e, e'). *Zeb2* inactivation also resulted in a substantial decrease in the number of Chx10-immunoreactive bipolar cells and PKCα-immunoreactive rod bipolar cells (Fig. 5f, f′; Fig. S2c, c′). In addition, it reduced neurons immunoreactive for Bhlhb5, a marker for Type 2 OFF-cone bipolar and GABAergic amacrine cells, as well as neurons immunoreactive for Isl1, a marker for bipolar, ganglion and cholinergic amacrine cells (Fig. 5g, g′; Fig. S2d, d′). There was less but significant loss of Müller cells immunoreactive for Sox9 and GS, and photoreceptor cells positive for recoverin in the $Zeb2^{\Delta fl/\Delta fl}$ retina (Fig. 5j, j′; Fig. S2f, g, f′, g′). Perhaps as a result of retinal degeneration, there was obvious gliosis in the mutant retina as determined by GFAP-immunoreactivity (Fig. S2 h, h′).

By quantifying immunoreactive cells, we found that in the $Zeb2^{\Delta fl/\Delta fl}$ retina, the number of $Chx10^+$, $PKC\alpha^+$, $Bhlhb5^+$ bipolar, $Bhlhb5^+$ amacrine, $Pax6^+$, $GAD65^+$, $Lim1^+$, $Brn3a^+$, $Brn3b^+$, and $Sox9^+$ cells was decreased by 30.0%, 43.8%, 83.2%, 39.9%, 56.1%, 62.0%, 77.4%, 57.3%, 58.4%, and 13.6%, respectively, compared to the control retina (Fig. 5k). So it appears that the $Bhlhb5^+$ Type 2 OFF-cone bipolar and

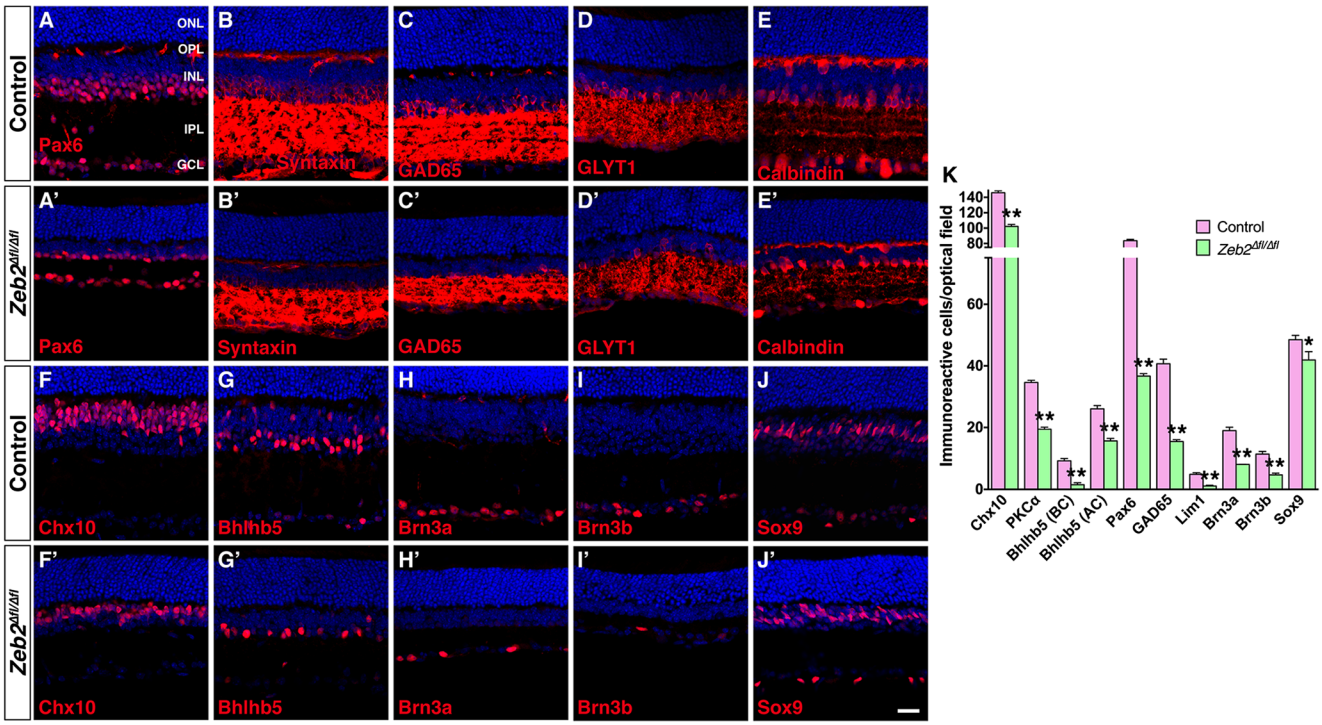

Fig. 5 Effect of *Zeb2* inactivation on the formation of non-photoreceptor retinal cell types. **a–j, a′–j′** Sections from P21 control and $Zeb2^{\Delta fl/\Delta fl}$ retinas were immunostained with antibodies against the indicated cell type-specific markers and weakly counterstained with nuclear DAPI. Loss of *Zeb2* function results in a decrease of amacrine cells immunoreactive for Pax6, syntaxin, Gad65, GLYT1, calbindin, or Bhlhb5 (**a–e**, **g**, **a′–e′**, **g′**), horizontal cells immunoreactive for calbindin (**e**, **e′**), bipolar cells immunoreactive for Chx10 or Bhlhb5 (**f**, **g**, **f′**, **g′**), ganglion cells immunoreactive for Brn3a, Brn3b, or Pax6 (**a**, **h**, **i**, **a′**, **h′**, **i′**), and Müller cells immunoreactive for Sox9 (**j**, **j′**). **k** Quantitation of cells that are immunoreactive for various cell type-specific markers in P21 control and $Zeb2^{\Delta fl/\Delta fl}$ retinas. Each histogram represents the mean ± SD for three retinas. $*p < 0.05$, $**p < 0.0005$. Abbreviations: GCL, ganglion cell layer; INL, inner nuclear layer; IPL, inner plexiform layer; ONL, outer nuclear layer; OPL, outer plexiform layer. Scale bar: **a–j**, **a′–j′**, 20 μm

horizontal cells are affected most and Müller cells are affected least by *Zeb2* inactivation. The sharp loss of Brn3a$^+$ and Brn3b$^+$ ganglion cells is consistent with the observed optic nerve hypoplasia associated with mutant mice (Fig. 4). These observed cell type losses in the *Zeb2*$^{\Delta fl/\Delta fl}$ retina thus suggest a requirement of Zeb2 in the generation, differentiation and/or maintenance of all non-photoreceptor retinal cell types.

The extensive loss of bipolar and horizontal cells in *Zeb2* mutant retinas may affect synaptic connections in the OPL. Indeed, peanut agglutinin (PNA) labeling revealed that flat contacts between cones and cone bipolar cells were diminished within the OPL in the P21 *Zeb2*$^{\Delta fl/\Delta fl}$ retina (Fig. S3a, b). Similarly, synaptic ribbons immunoreactive for Ribeye in the OPL became fewer in the mutant (Fig. S3c, d). Moreover, there was reduced staining for the synaptic vesicle marker synaptophysin in the mutant OPL (Fig. S3e, f). These results indicate a synaptogenic defect and/or loss of synaptic connections in the *Zeb2*$^{\Delta fl/\Delta fl}$ retina. Consistent with HE labeling and immunostaining for recoverin that showed shortened inner and outer segments of photoreceptors in the *Zeb2*$^{\Delta fl/\Delta fl}$ retina (Fig. 4j-m; Fig. S2 g, g'), PNA labeling specifically revealed that *Zeb2* ablation led to cones with shorter inner and outer segments as well (Fig. S3a, b), most likely as a result of the photoreceptor degeneration process.

To clarify the role of Zeb2 in early developmental events of non-photoreceptor cell types, we labeled P0 control and *Zeb2*$^{\Delta fl/\Delta fl}$ retinas with anti-Lim1 and anti-Tfap2a/2b antibodies to monitor horizontal and amacrine cells, and with anti-Brn3a and anti-Brn3b antibodies to monitor ganglion cells. In the *Zeb2*$^{\Delta fl/\Delta fl}$ retina at P0, we found an obvious decrease of horizontal cells immunoreactive for Lim1 or Tfap2a/2b and amacrine cells positive for Tfap2a/2b whereas the number of ganglion cells immunoreactive for Brn3a or Brn3b was similar between control and mutant retinas (Fig. S4a, b). For later-born cell types, we found overt reduction of Chx10-immunoreative bipolar cells in the P7 mutant retina whereas Sox9$^+$ Müller cells did not appear to change (Fig. S4a, b). These results are consistent with the previous observation that *Zeb2* ablation caused a decrease in the generation of horizontal, amacrine and bipolar cells but no reduction in the generation of ganglion and Müller cells [33]. Together, our data therefore suggest that Zeb2 is required for the specification of bipolar, amacrine and horizontal cells but not for the specification of ganglion and Müller cells and that it may be involved in the differentiation and maintenance of all non-photoreceptor cell types.

Impaired Electroretinogram (ERG) Responses in the *Zeb2* Mutant

To determine the effect of retinal defects on visual function in *Zeb2*$^{\Delta fl/\Delta fl}$ mice, we recorded ERG responses from 1-month and 6-month old control and *Zeb2*$^{\Delta fl/\Delta fl}$ animals. Under dark-adapted condition, for low flash intensities (0.003–0.03 cd.s/m^2), ERG responses were dominated by the b-wave, and mutant mice consistently showed lower response amplitudes than those elicited from control animals at both ages (Fig. 6a). For higher intensity flashes (0.1–10.0 cd.s/m^2), a-waves were visible for both control and mutant animals. When compared with control mice, the response amplitudes of a-waves elicited from mutant animals were reduced by approximately 55% at the age of 1 month and by about 80% at the age of 6 months (Fig. 6a, c). Similarly, the response amplitudes of b-waves elicited from mutant animals were reduced by approximately 75% at the age of 1 month and by about 90% at the age of 6 months (Fig. 6a, d). *Zeb2*$^{\Delta fl/\Delta fl}$ animals also showed a decrease in the amplitude of light-adapted ERG responses. Similar to scotopic ERG responses, under higher intensity flashes (3.0–30.0 cd.s/m^2), the response amplitudes of a-waves elicited from mutant animals were decreased by approximately 65% at the age of 1 month and by about 80% at the age of 6 months (Fig. 6b, e). Meanwhile, the response amplitudes of b-waves elicited from mutant animals were decreased by approximately 80% at the age of 1 month and by about 95% at the age of 6 months (Fig. 6b, f). The a- and b-waves are primarily generated by photoreceptors and bipolar cells, respectively [59–61]. Therefore, these results are consistent with the loss of all cell types including bipolar cells in the inner retinal layers, disrupted laminar retinal structure, retinal degeneration, and secondary degeneration of photoreceptors observed in *Zeb2*$^{\Delta fl/\Delta fl}$ mice.

Zeb2 Ablation Causes Cell Fate Switch to Photoreceptors

To explore the molecular basis underlying the regulatory role of Zeb2 in retinal development, we carried out RNA-seq analysis to identify genes differentially expressed in *Zeb2* mutant retinas. RNA was extracted from control and *Zeb2*$^{\Delta fl/\Delta fl}$ retinas at P0 when there was no extensive degeneration in the mutant retina. This analysis yielded 508 genes whose expression level is downregulated or upregulated by more than 1.5-fold in the mutant retina (Fig. 7a, b; Table S3). We performed gene set enrichment analysis (GSEA) of these altered genes followed by network visualization (Fig. 7c), which yielded a major clustered network of GO (gene ontology) terms for upregulated genes. These genes are enriched for biological process, cellular component, organophosphate metabolic process, and in particular, for visual perception and sensory perception of light stimulus. The group of upregulated genes enriched for visual perception includes many genes involved in phototransduction and photoreceptor function such as *rhodopsin (Rho), recoverin (Rcvrn), Gucy2e, Pde6b, Gnat1, Cnga1, Pdc, Rom1, Abca4*, and so on (Fig. 7d).

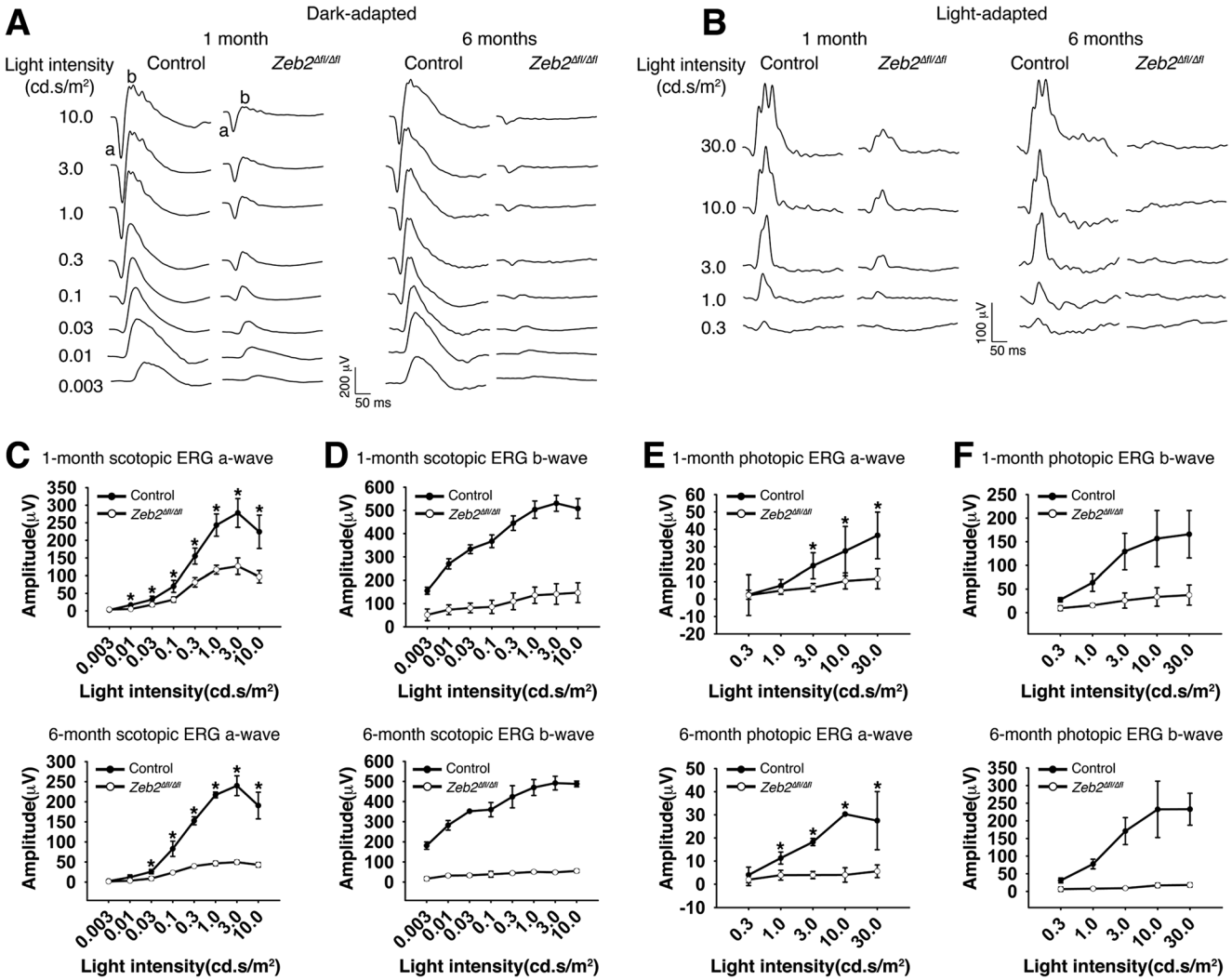

Fig. 6 ERG responses of *Zeb2* control and mutant mice. **a**, **b** Representative ERG waveforms from dark-adapted (**a**) or light-adapted (**b**) control and mutant animals aged 1 and 6 months. The flash intensities used to elicit the responses are indicated to the left. **c** Amplitudes of scotopic ERG a-waves elicited from control and $Zeb2^{\Delta fl/\Delta fl}$ mice aged 1 and 6 months. Asterisks denote statistically significant differences between control and mutant animals ($p < 0.02$). **d** Amplitudes of scotopic ERG b-waves elicited from control and $Zeb2^{\Delta fl/\Delta fl}$ mice aged 1 and 6 months. Differences between control and mutant animals are significant ($p < 0.0005$) at all flash intensities. **e** Amplitudes of photopic ERG a-waves elicited from control and $Zeb2^{\Delta fl/\Delta fl}$ mice aged 1 and 6 months. Asterisks denote statistically significant differences between control and mutant animals ($p < 0.04$). **f** Amplitudes of photopic ERG b-waves elicited from control and $Zeb2^{\Delta fl/\Delta fl}$ mice aged 1 and 6 months. Differences between control and mutant animals are significant ($p < 0.02$) at all flash intensities

We carried out qRT-PCR assay to validate upregulation of photoreceptor gene expression in P0 $Zeb2^{\Delta fl/\Delta fl}$ retinas. In agreement with the RNA-seq data, there is a significant increase in the expression of *Abca4*, *Rho, Rcvrn, Gucy2e, Pde6b, Pde6c, Pde6g, Pde6h, Gnat1, Cnga1, Pdc, Rom1* in the mutant retina (Fig. 7e). Moreover, the expression of *Crx*, *Nrl* and *Nr2e3*, all transcription factor genes involved in photoreceptor specification and differentiation [62–66], is also significantly upregulated (Fig. 7e). Immunolabeling confirmed the presence of increased recoverin-, Nr2e3- and Rxrg-immunoreactive cells at the outer edge of the mutant retina compared to the control (Fig. 7f). In addition, some rhodopsin-positive cells appeared in the outer edge of the mutant retina whereas there was a complete absence of these cells in the control (Fig. 7f). The increased or precocious expression of many photoreceptor genes in P0 $Zeb2^{\Delta fl/\Delta fl}$ retinas thus suggests that *Zeb2* inactivation may result in a cell fate change of retinal progenitors to photoreceptors.

Zeb2 Misexpression Promotes the Differentiation of All Non-photoreceptor Cell Types

Given the necessity for Zeb2 in controlling development of all cell types in the inner retinal layers, we assessed its sufficiency to promote non-photoreceptor cell differentiation. We thus overexpressed Zeb2 in the mouse retina using the pCIG expression vector carrying a GFP reporter [54, 55, 67]. pCIG-Zeb2 and pCIG plasmid DNA (Fig.

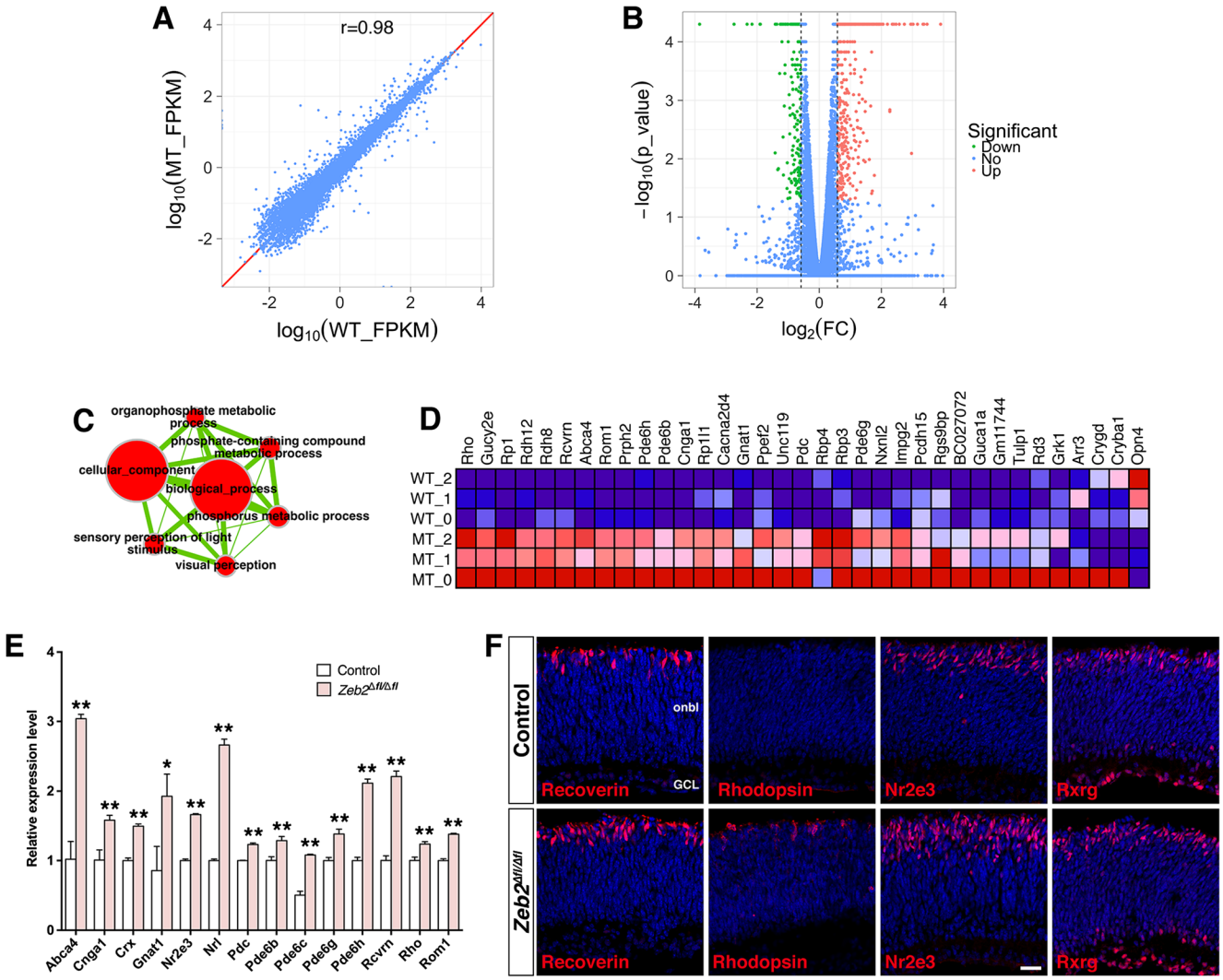

Fig. 7 RNA-seq analysis of differentially expressed genes in P0 *Zeb2* mutant retinas. **a** Scatter plot of global gene expression profiles. Gene expression levels (FPKM) are depicted in $\log_{10}$ scale. The diagonal line represents equal expression in the two genotypes (WT, wild type; MT, mutant). The Pearson correlation coefficient is indicated. **b** Volcano plot (significance vs fold change) of significantly downregulated (green) and upregulated (red) genes (fold change ≥ 1.5 and $p < 0.05$) between the wild type and mutant retinas. **c** Gene ontology (GO) enrichment analysis of the altered genes between *Zeb2* wild type and mutant retinas. The altered genes were analyzed for GO term enrichment by gene set enrichment analysis (GSEA). The result was visualized on a network of gene-sets (nodes) connected by their similarity (edges). Node size represents the gene-set size and edge thickness represents the degree of overlap between two gene sets. **d** GSEA output heatmap of expression levels for the set of altered genes enriched for visual perception. **e** Relative mRNA levels of the indicated genes determined by qRT-PCR analysis. Each histogram represents the mean ± SD ($n = 3$). *$p < 0.05$, **$p < 0.005$. **f** P0 retinal sections from control and $Zeb2^{\Delta fl/\Delta fl}$ neonates were immunostained with the indicated antibodies and weakly counterstained with nuclear DAPI. There is increase in the number of recoverin-, rhodopsin-, Nr2e3- and Rxrg-immunoreactive cells in the mutant retina. Abbreviations: GCL, ganglion cell layer; onbl, outer neuroblastic layer. Scale bar: **f**, 20 μm

S5a) was injected into the subretinal space of newborn mice and electroporated into the retina. At P12, we analyzed the laminar position and morphology of GFP^+ cells in transfected retinas. In retinas transfected with pCIG-Zeb2 DNA, the fraction of GFP^+ cells differentiated as photoreceptors in the ONL dropped from 82.8% in the control retina to 76.9% (Fig. S5b-d). In contrast, the fraction of GFP^+ cells distributed in the INL increased from 17.2% in the control to 23.1% (Fig. S5b-d). Thus, Zeb2 misexpression substantially changes the proportions of progeny distributed in different retinal cell layers.

The increased GFP^+ cells in the INL of retinas transfected with the pCIG-Zeb2 plasmid could represent more amacrine, horizontal, bipolar, and/or Müller cells. To distinguish these possibilities, we used a series of cell type-specific markers to analyze the types of GFP^+ cells. First, we found that ectopically expressed Zeb2 appeared to increase the number of GFP^+ cells immunoreactive for Chx10, PKCα and Bhlhb5, which are proteins expressed in bipolar cells (Fig. 8a–c, a′–c′). Quantification of colocalized cells revealed that forced Zeb2 expression significantly increased the percentage of $Chx10^+$ bipolar cells from 3.7 to 6.2%, $PKC\alpha^+$ rod bipolar cells from

1.1 to 1.6%, and Bhlhb5$^+$ type 2 OFF-cone bipolar cells from 0.7 to 0.9% (Fig. 8l). Second, overexpressed Zeb2 significantly increased the proportion of Pax6$^+$ amacrine cells from 5.3 to 10.4%, GLYT1$^+$ glycinergic amacrine cells from 2.1 to 4.3%, Gad65$^+$ GABAergic amacrine cells from 1.0 to 3.6%, and Bhlhb5$^+$ GABAergic amacrine cells from 1.1 to 4.1% (Fig. 8c–f, c′–f′, l). Third, in retinas transfected with the pCIG-Zeb2 plasmid, there was approximately 2-fold increase in the fraction of GFP$^+$ cells differentiated as Sox9$^+$ Müller cells (Fig. 8g, g′, l). Finally, contrary to cell types in the INL, Zeb2 overexpression caused a significant reduction of recoverin$^+$ photoreceptors from 74.2 to 57.7% (Fig. 8h, h′, l), in agreement with the observed photoreceptor increase in *Zeb2*$^{\Delta fl/\Delta fl}$ retinas (Fig. 7). These data suggest that Zeb2 is capable of promoting the differentiation of bipolar, amacrine and Müller cells at the expense of photoreceptors.

To determine the effect of misexpressed Zeb2 on development of ganglion and horizontal cells, which are born at embryonic stages, we electroporated ex vivo pCIG-Zeb2 and pCIG plasmid DNA into the E14.5 retina. Following a 4.5-day culture of the electroporated eyecups, we harvested the infected retinas to analyze differentiation of ganglion and horizontal cells. We found that misexpressed Zeb2 increased Brn3a$^+$ ganglion cells from 3.3 to 5.0%, Brn3b$^+$ ganglion cells from 2.2 to 5.3%, and Lim1$^+$ horizontal cells from 0.9% to 1.5 (Fig. 8i–k, i′–k′, m). Therefore, these data together suggest that Zeb2 has the ability to promote differentiation of all non-photoreceptor cell types including bipolar, amacrine, horizontal, ganglion, and Müller cells which are normally distributed in the INL and GCL.

Discussion

In this study, we show that Zeb2 is expressed transiently in early retinal progenitors and in all non-photoreceptor cell types and that it plays a crucial role in modulating development of all these cell types (Fig. 9). Conditional inactivation of *Zeb2* in the mouse retina causes age-dependent retinal degeneration, reduced optic nerve size, synaptic connection defects, and impaired visual responses as a result of severe loss of non-photoreceptor cells, cell fate change to photoreceptors by retinal progenitors, and increased apoptotic cell death. The cell fate change seen in the mutant retina appears to result from dysregulation in the expression of transcription factor genes involved in photoreceptor specification and differentiation, which are normally repressed by Zeb2 (Fig. 9). The age-dependent degeneration of both non-photoreceptor and photoreceptor cells and deteriorating ERG responses seen in mutant mice suggest that Zeb2 is also directly and or/indirectly required for the long-term maintenance of all retinal cell types and structure. Furthermore, we show that forced Zeb2 expression is sufficient to promote the fate of all non-photoreceptor cells at the expense of photoreceptors. Because early generation of bipolar, amacrine and horizontal cells is impaired whereas that of ganglion and Müller cells is not in the *Zeb2* mutant retina, Zeb2 may be both necessary and sufficient for the specification, differentiation and maintenance of bipolar, amacrine and horizontal cells. In contrast, it may be necessary and sufficient for the differentiation and maintenance of ganglion and Müller cells but unnecessary for their specification.

While our study on the role of Zeb2 in retinal development was ongoing, a retina-specific knockout analysis of *Zeb2/Sip1* function was reported [33]. Despite some similar and consistent conclusions reached by both studies, this work provides several novel insights and make several clarifications compared to the previous one:

1) It was reported in the previous study that Zeb2 was not expressed in bipolar or Müller cells but displayed non-nuclear synaptic expression in the OPL of the retina [33]. We found that Zeb2 is expressed in about 40% of bipolar cells including both rod and cone bipolar cells and that there is an increase of Zeb2-positive rod bipolar cells from P12 to P21 (Fig. 3). Similarly, Zeb2 is present in the great majority of Müller cells. There is no specific expression of Zeb2 in the OPL, which can be corroborated by both RNA in situ hybridization and immunostaining (Figs. 2, 3). The distribution of Zeb2 in all non-photoreceptor cell types is more consistent with the observed effect of *Zeb2* knockout and overexpression on all cell types located within inner retinal layers including bipolar, amacrine, horizontal, Müller, and ganglion cells. One possible explanation for the immunolabeling discrepancy between this and previous studies might be the fixation time of the retinal tissue because only when we fixed the retina for a shorter time (10 min) did the synaptic labeling disappear.
2) We utilized the Six3-Cre transgenic mouse line, which drives Cre expression in all retinal progenitors [39], to conditionally ablate *Zeb2* in the entire retina, whereas the Pax6 α-Cre transgenic line was used to inactivate *Zeb2* only in the distal retina in the previous work [33]. This difference has provided us with the advantage to better model and recapitulate the structural ocular defects observed in the Mowat-Wilson syndrome patients, such as optic nerve hypoplasia which was not observed in the prior study [33]. It has also enabled us to detect more severe ERG response defects in *Zeb2* mutant mice and increased severeness in ERG response and retinal laminar defects in mutants from 1 to 6 months, hence revealing that *Zeb2* inactivation leads to not only cell specification defects but also retinal degeneration including gradual loss of photoreceptors, whereas in the previous study photoreceptor degeneration was unseen in the mutant [33]. Retinal degeneration in *Zeb2* mutants may result from

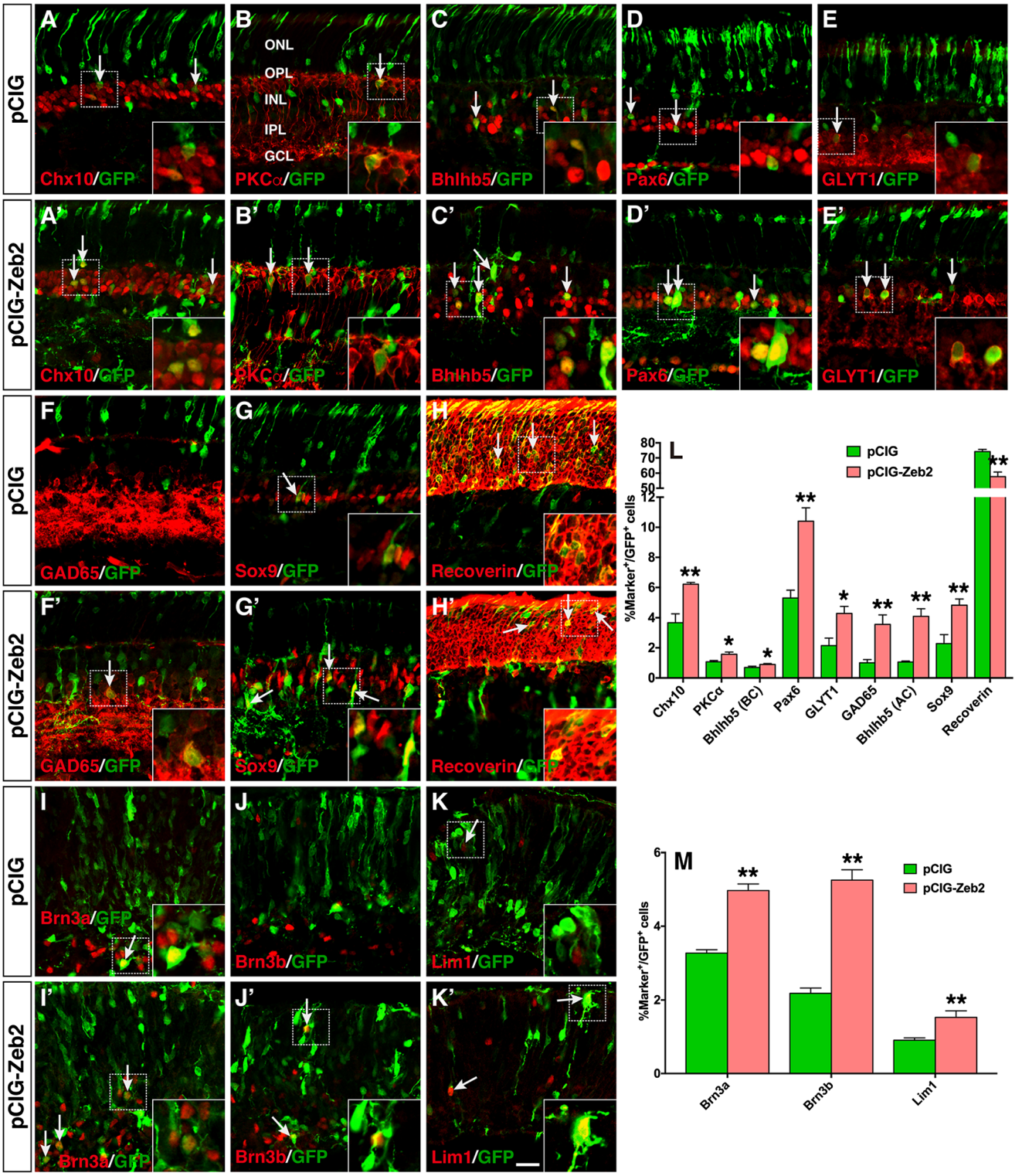

direct loss of all cell types in the inner retinal layers, in particular bipolar and horizontal cells. For instance, failure to generate horizontal cells or their ablation results in degeneration of all retinal cell types [68–70].

3) This work reveals that *Zeb2* inactivation may cause a cell fate switch of retinal progenitors to photoreceptors, a phenomenon not observed in the previous knockout study [33]. As determined by RNA-seq, qRT-PCR and immunolabeling analyses, the generation of supernumerary photoreceptors in neonatal $Zeb2^{\Delta fl/\Delta fl}$ retinas was supported by increased or precocious expression of many genes involved in the development, phototransduction

◀ **Fig. 8** Effect of misexpressed Zeb2 on the formation of different retinal cell types. **a–h**, **a′–h′** Neonatal retinas were electroporated in vivo with pCIG or pCIG-Zeb2 DNA, collected at P12, then their sections were double-immunostained with an anti-GFP antibody and antibodies against the indicated cell type-specific markers. Misexpressed Zeb2 resulted in an increase in the number of cells immunoreactive for Chx10, PKCα, Bhlhb5, Pax6, GLYT1, Gad65, or Sox9, but suppressed the formation of photoreceptor cells immunoreactive for recoverin. Arrows point to representative colocalized cells and insets show corresponding outlined regions at a higher magnification. **i–k**, **i′–k′** E14.5 retinas were electroporated ex vivo with pCIG or pCIG-Zeb2 DNA, collected after a 4-day culture, then their sections were double-immunostained with an anti-GFP antibody and antibodies against Brn3a, Brn3b, or Lim1. Misexpressed Zeb2 increased cells immunoreactive for Brn3a, Brn3b, or Lim1. Arrows point to representative colocalized cells and insets show corresponding outlined regions at a higher magnification. **l** Quantitation of GFP^+ cells that become immunoreactive for a series of cell type-specific markers, in retinas electroporated at P0. Each histogram represents the mean ± SD for three retinas. More than 720 GFP^+ cells were scored in each retina. $*p < 0.05$, $**p < 0.005$. **m** Quantitation of GFP^+ cells that become immunoreactive for Brn3a, Brn3b, or Lim1, in retinas electroporated at E14.5. Each histogram represents the mean ± SD for three retinas. More than 1000 GFP^+ cells were scored in each retina. $**p < 0.005$. Abbreviations: AC, amacrine cell; BC, bipolar cell; GCL, ganglion cell layer; INL, inner nuclear layer; IPL, inner plexiform layer; ONL, outer nuclear layer; OPL, outer plexiform layer. Scale bar: **a–k**, **a′–k′**, 20 μm

and physiological function of photoreceptors. As such, it appears that Zeb2 is required not only for promoting the differentiation of non-photoreceptor cells but also for simultaneously inhibiting the photoreceptor cell fate by repressing the expression of *Crx*, *Nrl* and *Nr2e3*, which are transcription factor genes involved in photoreceptor specification and differentiation [62–66]. It should be noted that although the evidence for a cell fate switch in the $Zeb2^{\Delta fl/\Delta fl}$ retina is strong and likely, direct evidence is lacking and would require additional lineage tracing experiments.

4) Our study determined the sufficiency of Zeb2 in development of non-photoreceptor cells by misexpression of Zeb2 in neonatal and embryonic retinas, which promoted the differentiation of bipolar, amacrine, horizontal, Müller, and ganglion cells. Therefore, Zeb2 is both necessary and sufficient for promoting the differentiation of all non-photoreceptor cell types during retinal development. Gain-of-function experiments were not performed in the previous study [33].
5) In this study, our overexpression experiments with Zeb2 demonstrated that it is capable of promoting the differentiation of retinal ganglion and Müller cells. And our conditional knockout experiments showed that there is a significant loss of ganglion and Müller cells in *Zeb2* mutant retinas by P21 even though their initial generation is unaffected. Ganglion cell loss is also consistent with the

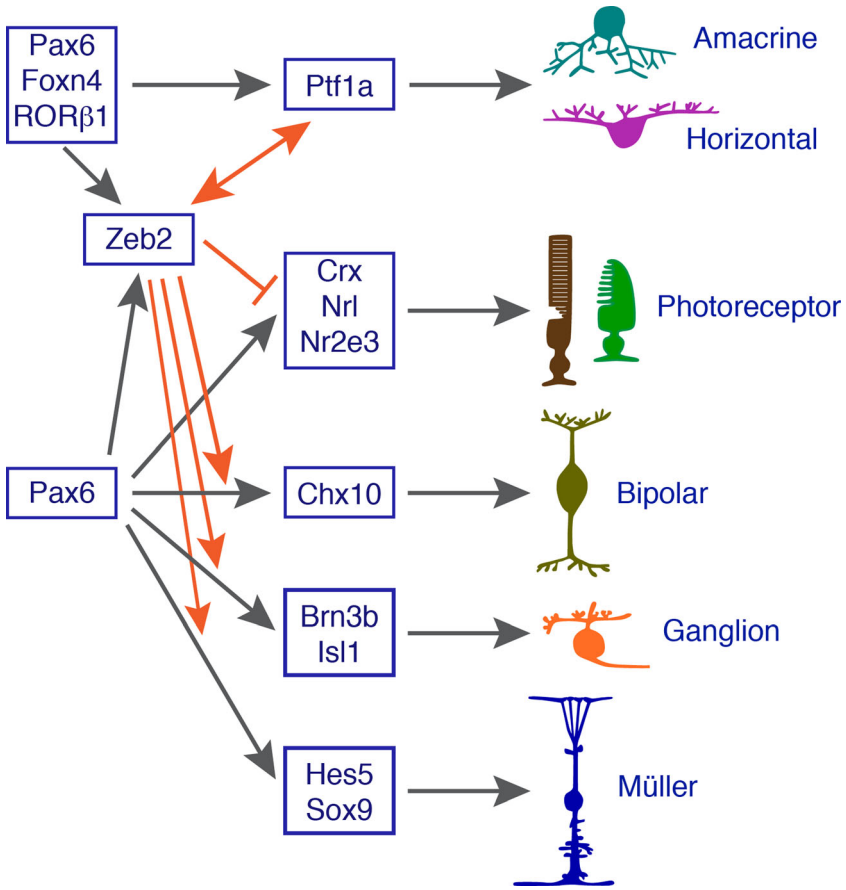

Fig. 9 Working model by which Zeb2 participates in the specification, differentiation and maintenance of non-photoreceptor cells during retinal development. Zeb2 may be both necessary and sufficient for the specification, differentiation and maintenance of bipolar, amacrine and horizontal cells. By contrast, it may be necessary and sufficient for the differentiation and maintenance of ganglion and Müller cells but unnecessary for their specification. Zeb2 acts downstream of Pax6 to promote the differentiation and survival of non-photoreceptor cells. Zeb2 and Ptf1a may activate gene expression of each other to control amacrine and horizontal cell differentiation. While regulating non-photoreceptor cell development, Zeb2 simultaneously suppresses the photoreceptor cell fate by inhibiting the expression of photoreceptor transcriptional regulators Crx, Nrl, and Nr2e3

observed optic nerve hypoplasia and optic disc swelling in *Zeb2*$^{\Delta fl/\Delta fl}$ mice. Thus, Zeb2 may be both necessary and sufficient for the differentiation and maintenance of ganglion and Müller cells despite the lack of requirement of it in the specification of these two cell types. As for bipolar, amacrine and horizontal cells, because of their early defects in the *Zeb2*$^{\Delta fl/\Delta fl}$ retina, Zeb2 is likely involved in the specification, differentiation and maintenance of these three cell types. Our work therefore provides a much more thorough understanding of Zeb2 function during retinal development than the previous study [33].

In retinal development, Zeb2 has been shown to function downstream of Pax6, a key transcriptional regulator conferring retinal progenitors with multipotency [33]. It also binds to the *Ptf1a* 3′ enhancer to activate its expression [33], indicating that Zeb2 acts upstream of Ptf1a to regulate amacrine and horizontal cell development. However, our microarray data show that the expression of *Zeb2* is downregulated in *Ptf1a* mutant retinas, suggesting that *Zeb2* and *Ptf1a* may cross-activate the expression of each other to control amacrine and horizontal cell specification (Fig. 9). It appears that Zeb2 is not required for the maintenance of *Ptf1a* expression since in *Zeb2*$^{\Delta fl/\Delta fl}$ retinas *Ptf1a* expression is not abolished—only the onset of its expression is delayed [33].

Mowat-Wilson syndrome is a monogenic congenital disorder often diagnosed in infants and children. The prevalence of structural ocular defects in this syndrome has not been recognized until recently and is thought to be significantly underestimated [15, 21–23]. One reason may be that retinal coloboma has a more complex etiology than other tissue anomalies in patients and may manifest at a different age range. Currently, Mowat-Wilson syndrome is considered as an early developmental disease. Previous molecular and cellular studies including *Zeb2* knockout analyses are all based on this assumption, providing evidence for the requirement of Zeb2 in patterning neural and lens epithelia, neural tube closure, specification and differentiation of neural crest cells and neurons, and migration of neural crest and cortical cells [27–32]. However, our results show the expression of Zeb2 in retinal progenitors, differentiating cells, as well as in mature cells of the adult mouse retina. Moreover, its retina-specific inactivation resulted in retinal cell loss and severe age-dependent retinal thinning and visual impairment. Based on these observations, we speculate that in addition to a role in the specification and differentiation of non-photoreceptor cells, another important function of Zeb2 in the retina is to control the long-term survival of these cells. This postulation is in no contradiction with the developmental nature of the Mowat-Wilson syndrome, but rather suggests that it may be additionally considered as a degenerative retinal disease. Our hypothesis implicates a previously unrecognized etiology of retinal coloboma associated with Mowat-Wilson syndrome and that a patient's eye phenotype may not completely manifest until an older age. This suggests that it may be necessary for ophthalmologists to check and evaluate the progression of retinal atrophy in adult Mowat-Wilson syndrome patients on a regular basis. Thus, our current studies are expected to make a significant impact not only on understanding the general mechanism of retinal neurogenesis and maintenance but also on clinical diagnosis and management of Mowat-Wilson syndrome patients.

Acknowledgements We thank Drs. Chuang Shen and Shuting Liu for critical reading of and thoughtful comments on the manuscript. This work was supported in part by the National Key R&D Program of China (2017YFA0104100), National Basic Research Program (973 Program) of China (2015CB964600), National Natural Science Foundation of China (81670862), Science and Technology Planning Projects of Guangdong Province (2017B030314025), National Institutes of Health (EY020849 and EY012020), and the Fundamental Research Funds of the State Key Laboratory of Ophthalmology, Sun Yat-sen University to MX.

References

1. Livesey FJ, Cepko CL (2001) Vertebrate neural cell-fate determination: lessons from the retina. Nat Rev Neurosci 2(2):109–118
2. Harris WA (1997) Cellular diversification in the vertebrate retina. Curr Opin Genet Dev 7(5):651–658
3. Xiang M (2013) Intrinsic control of mammalian retinogenesis. Cell Mol Life Sci 70(14):2519–2532. https://doi.org/10.1007/s00018-012-1183-2
4. Yang XJ (2004) Roles of cell-extrinsic growth factors in vertebrate eye pattern formation and retinogenesis. Semin Cell Dev Biol 15(1):91–103. https://doi.org/10.1016/j.semcdb.2003.09.004
5. Boije H, MacDonald RB, Harris WA (2014) Reconciling competence and transcriptional hierarchies with stochasticity in retinal lineages. Curr Opin Neurobiol 27:68–74. https://doi.org/10.1016/j.conb.2014.02.014
6. Agathocleous M, Harris WA (2009) From progenitors to differentiated cells in the vertebrate retina. Annu Rev Cell Dev Biol 25:45–69. https://doi.org/10.1146/annurev.cellbio.042308.113259
7. Swaroop A, Kim D, Forrest D (2010) Transcriptional regulation of photoreceptor development and homeostasis in the mammalian retina. Nat Rev Neurosci 11(8):563–576. https://doi.org/10.1038/nrn2880
8. Cronin T, Leveillard T, Sahel JA (2007) Retinal degenerations: from cell signaling to cell therapy; pre-clinical and clinical issues. Curr Gene Ther 7(2):121–129
9. Fitzpatrick DR, van Heyningen V (2005) Developmental eye disorders. Curr Opin Genet Dev 15(3):348–353. https://doi.org/10.1016/j.gde.2005.04.013
10. Zagozewski JL, Zhang Q, Eisenstat DD (2014) Genetic regulation of vertebrate eye development. Clin Genet 86(5):453–460. https://doi.org/10.1111/cge.12493
11. Espinosa-Parrilla Y, Amiel J, Auge J, Encha-Razavi F, Munnich A, Lyonnet S, Vekemans M, Attie-Bitach T (2002) Expression of the SMADIP1 gene during early human development. Mech Dev 114(1–2):187–191
12. Verschueren K, Remacle JE, Collart C, Kraft H, Baker BS, Tylzanowski P, Nelles L, Wuytens G et al (1999) SIP1, a novel zinc finger/homeodomain repressor, interacts with Smad proteins and binds to 5'-CACCT sequences in candidate target genes. J Biol Chem 274(29):20489–20498

13. Postigo AA, Dean DC (2000) Differential expression and function of members of the zfh-1 family of zinc finger/homeodomain repressors. Proc Natl Acad Sci U S A 97(12):6391–6396
14. Yamada Y, Nomura N, Yamada K, Matsuo M, Suzuki Y, Sameshima K, Kimura R, Yamamoto Y et al (2014) The spectrum of ZEB2 mutations causing the Mowat-Wilson syndrome in Japanese populations. Am J Med Genet A 164A(8):1899–1908. https://doi.org/10.1002/ajmg.a.36551
15. Wenger TL, Harr M, Ricciardi S, Bhoj E, Santani A, Adam MP, Barnett SS, Ganetzky R et al (2014) CHARGE-like presentation, craniosynostosis and mild Mowat-Wilson syndrome diagnosed by recognition of the distinctive facial gestalt in a cohort of 28 new cases. Am J Med Genet A 164A(10):2557–2566. https://doi.org/10.1002/ajmg.a.36696
16. Ghoumid J, Drevillon L, Alavi-Naini SM, Bondurand N, Rio M, Briand-Suleau A, Nasser M, Goodwin L et al (2013) ZEB2 zinc-finger missense mutations lead to hypomorphic alleles and a mild Mowat-Wilson syndrome. Hum Mol Genet 22(13):2652–2661. https://doi.org/10.1093/hmg/ddt114
17. Garavelli L, Mainardi PC (2007) Mowat-Wilson syndrome. Orphanet J Rare Dis 2:42. https://doi.org/10.1186/1750-1172-2-42
18. Zweier C, Thiel CT, Dufke A, Crow YJ, Meinecke P, Suri M, Ala-Mello S, Beemer F et al (2005) Clinical and mutational spectrum of Mowat-Wilson syndrome. Eur J Med Genet 48(2):97–111. https://doi.org/10.1016/j.ejmg.2005.01.003
19. Wakamatsu N, Yamada Y, Yamada K, Ono T, Nomura N, Taniguchi H, Kitoh H, Mutoh N et al (2001) Mutations in SIP1, encoding Smad interacting protein-1, cause a form of Hirschsprung disease. Nat Genet 27(4):369–370. https://doi.org/10.1038/86860
20. Gregory-Evans CY, Vieira H, Dalton R, Adams GG, Salt A, Gregory-Evans K (2004) Ocular coloboma and high myopia with Hirschsprung disease associated with a novel ZFHX1B missense mutation and trisomy 21. Am J Med Genet A 131(1):86–90. https://doi.org/10.1002/ajmg.a.30312
21. Tanteles GA, Christophidou-Anastasiadou V (2014) Ocular phenotype of Mowat-Wilson syndrome in the first reported Cypriot patients: an under-recognized association. Clin Dysmorphol 23(1):20–23. https://doi.org/10.1097/MCD.0000000000000013
22. Ariss M, Natan K, Friedman N, Traboulsi EI (2012) Ophthalmologic abnormalities in Mowat-Wilson syndrome and a mutation in ZEB2. Ophthalmic Genet 33(3):159–160. https://doi.org/10.3109/13816810.2011.610860
23. Dastot-Le Moal F, Wilson M, Mowat D, Collot N, Niel F, Goossens M (2007) ZFHX1B mutations in patients with Mowat-Wilson syndrome. Hum Mutat 28(4):313–321. https://doi.org/10.1002/humu.20452
24. McGaughran J, Sinnott S, Dastot-Le Moal F, Wilson M, Mowat D, Sutton B, Goossens M (2005) Recurrence of Mowat-Wilson syndrome in siblings with the same proven mutation. Am J Med Genet A 137A(3):302–304. https://doi.org/10.1002/ajmg.a.30896
25. Hurst JA, Markiewicz M, Kumar D, Brett EM (1988) Unknown syndrome: Hirschsprung's disease, microcephaly, and iris coloboma: a new syndrome of defective neuronal migration. J Med Genet 25(7):494–497
26. Khor CC, Miyake M, Chen LJ, Shi Y, Barathi VA, Qiao F, Nakata I, Yamashiro K et al (2013) Genome-wide association study identifies ZFHX1B as a susceptibility locus for severe myopia. Hum Mol Genet 22(25):5288–5294. https://doi.org/10.1093/hmg/ddt385
27. Miquelajauregui A, Van de Putte T, Polyakov A, Nityanandam A, Boppana S, Seuntjens E, Karabinos A, Higashi Y et al (2007) Smad-interacting protein-1 (Zfhx1b) acts upstream of Wnt signaling in the mouse hippocampus and controls its formation. Proc Natl Acad Sci U S A 104(31):12919–12924. https://doi.org/10.1073/pnas.0609863104
28. Van de Putte T, Maruhashi M, Francis A, Nelles L, Kondoh H, Huylebroeck D, Higashi Y (2003) Mice lacking ZFHX1B, the gene that codes for Smad-interacting protein-1, reveal a role for multiple neural crest cell defects in the etiology of Hirschsprung disease-mental retardation syndrome. Am J Hum Genet 72(2):465–470. https://doi.org/10.1086/346092
29. Yoshimoto A, Saigou Y, Higashi Y, Kondoh H (2005) Regulation of ocular lens development by Smad-interacting protein 1 involving Foxe3 activation. Development 132(20):4437–4448. https://doi.org/10.1242/dev.02022
30. Seuntjens E, Nityanandam A, Miquelajauregui A, Debruyn J, Stryjewska A, Goebbels S, Nave KA, Huylebroeck D et al (2009) Sip1 regulates sequential fate decisions by feedback signaling from postmitotic neurons to progenitors. Nat Neurosci 12(11):1373–1380. https://doi.org/10.1038/nn.2409
31. van den Berghe V, Stappers E, Vandesande B, Dimidschstein J, Kroes R, Francis A, Conidi A, Lesage F et al (2013) Directed migration of cortical interneurons depends on the cell-autonomous action of Sip1. Neuron 77(1):70–82. https://doi.org/10.1016/j.neuron.2012.11.009
32. Van de Putte T, Francis A, Nelles L, van Grunsven LA, Huylebroeck D (2007) Neural crest-specific removal of Zfhx1b in mouse leads to a wide range of neurocristopathies reminiscent of Mowat-Wilson syndrome. Hum Mol Genet 16(12):1423–1436. https://doi.org/10.1093/hmg/ddm093
33. Menuchin-Lasowski Y, Oren-Giladi P, Xie Q, Ezra-Elia R, Ofri R, Peled-Hajaj S, Farhy C, Higashi Y et al (2016) Sip1 regulates the generation of the inner nuclear layer retinal cell lineages in mammals. Development 143(15):2829–2841. https://doi.org/10.1242/dev.136101
34. Fujitani Y, Fujitani S, Luo H, Qiu F, Burlison J, Long Q, Kawaguchi Y, Edlund H et al (2006) Ptf1a determines horizontal and amacrine cell fates during mouse retinal development. Development 133(22):4439–4450
35. Li S, Mo Z, Yang X, Price SM, Shen MM, Xiang M (2004) Foxn4 controls the genesis of amacrine and horizontal cells by retinal progenitors. Neuron 43(6):795–807
36. Jin K, Jiang H, Xiao D, Zou M, Zhu J, Xiang M (2015) Tfap2a and 2b act downstream of Ptf1a to promote amacrine cell differentiation during retinogenesis. Mol Brain 8:28. https://doi.org/10.1186/s13041-015-0118-x
37. Watanabe S, Sanuki R, Sugita Y, Imai W, Yamazaki R, Kozuka T, Ohsuga M, Furukawa T (2015) Prdm13 regulates subtype specification of retinal amacrine interneurons and modulates visual sensitivity. J Neurosci 35(20):8004–8020. https://doi.org/10.1523/JNEUROSCI.0089-15.2015
38. Higashi Y, Maruhashi M, Nelles L, Van de Putte T, Verschueren K, Miyoshi T, Yoshimoto A, Kondoh H et al (2002) Generation of the floxed allele of the SIP1 (Smad-interacting protein 1) gene for Cre-mediated conditional knockout in the mouse. Genesis 32(2):82–84
39. Furuta Y, Lagutin O, Hogan BL, Oliver GC (2000) Retina- and ventral forebrain-specific Cre recombinase activity in transgenic mice. Genesis 26(2):130–132. https://doi.org/10.1002/(SICI)1526-968X(200002)26:2<130::AID-GENE9>3.0.CO;2-I
40. Qiu F, Jiang H, Xiang M (2008) A comprehensive negative regulatory program controlled by Brn3b to ensure ganglion cell specification from multipotential retinal precursors. J Neurosci 28(13):3392–3403. https://doi.org/10.1523/JNEUROSCI.0043-08.2008
41. Kawaguchi Y, Cooper B, Gannon M, Ray M, MacDonald RJ, Wright CV (2002) The role of the transcriptional regulator Ptf1a in converting intestinal to pancreatic progenitors. Nat Genet 32(1):128–134. https://doi.org/10.1038/ng959
42. Li C, Wong WH (2003) DNA-Chip analyzer (dChip). In: Parmigiani G, Garrett ES, Irizarry R, Zeger SL (eds) The analysis of gene expression data: methods and software. Springer-Verlag, New York, pp. 120–141
43. Subramanian A, Tamayo P, Mootha VK, Mukherjee S, Ebert BL, Gillette MA, Paulovich A, Pomeroy SL et al (2005) Gene set

enrichment analysis: a knowledge-based approach for interpreting genome-wide expression profiles. Proc Natl Acad Sci U S A 102(43):15545–15550. https://doi.org/10.1073/pnas.0506580102
44. Cline MS, Smoot M, Cerami E, Kuchinsky A, Landys N, Workman C, Christmas R, Avila-Campilo I et al (2007) Integration of biological networks and gene expression data using Cytoscape. Nat Protoc 2(10):2366–2382. https://doi.org/10.1038/nprot.2007.324
45. Merico D, Isserlin R, Stueker O, Emili A, Bader GD (2010) Enrichment map: a network-based method for gene-set enrichment visualization and interpretation. PLoS One 5(11):e13984. https://doi.org/10.1371/journal.pone.0013984
46. Sciavolino PJ, Abrams EW, Yang L, Austenberg LP, Shen MM, Abate-Shen C (1997) Tissue-specific expression of murine Nkx3.1 in the male urogenital system. Dev Dyn 209(1):127–138
47. Mo Z, Li S, Yang X, Xiang M (2004) Role of the Barhl2 homeobox gene in the specification of glycinergic amacrine cells. Development 131(7):1607–1618
48. Hodges RS, Heaton RJ, Parker JM, Molday L, Molday RS (1988) Antigen-antibody interaction. Synthetic peptides define linear antigenic determinants recognized by monoclonal antibodies directed to the cytoplasmic carboxyl terminus of rhodopsin. J Biol Chem 263(24):11768–11775
49. Yang S, Luo X, Xiong G, So KF, Yang H, Xu Y (2015) The electroretinogram of Mongolian gerbil (Meriones unguiculatus): comparison to mouse. Neurosci Lett 589:7–12. https://doi.org/10.1016/j.neulet.2015.01.018
50. Wu XH, Qian KW, Xu GZ, Li YY, Ma YY, Huang F, Wang YQ, Zhou X et al (2016) The role of retinal dopamine in C57BL/6 mouse refractive development as revealed by intravitreal administration of 6-hydroxydopamine. Invest Ophthalmol Vis Sci 57(13):5393–5404. https://doi.org/10.1167/iovs.16-19543
51. Pfaffl MW (2001) A new mathematical model for relative quantification in real-time RT-PCR. Nucleic Acids Res 29(9):e45
52. Irie S, Sanuki R, Muranishi Y, Kato K, Chaya T, Furukawa T (2015) Rax homeoprotein regulates photoreceptor cell maturation and survival in association with Crx in the postnatal mouse retina. Mol Cell Biol 35(15):2583–2596. https://doi.org/10.1128/MCB.00048-15
53. Mansergh FC, Carrigan M, Hokamp K, Farrar GJ (2015) Gene expression changes during retinal development and rod specification. Mol Vis 21:61–87
54. Megason SG, McMahon AP (2002) A mitogen gradient of dorsal midline Wnts organizes growth in the CNS. Development 129(9):2087–2098
55. Jin K, Jiang H, Mo Z, Xiang M (2010) Early B-cell factors are required for specifying multiple retinal cell types and subtypes from postmitotic precursors. J Neurosci 30(36):11902–11916. https://doi.org/10.1523/JNEUROSCI.2187-10.2010
56. Kuwajima T, Soares CA, Sitko AA, Lefebvre V, Mason C (2017) SoxC transcription factors promote contralateral retinal ganglion cell differentiation and axon guidance in the mouse visual system. Neuron 93(5):1110–1125 e1115. https://doi.org/10.1016/j.neuron.2017.01.029
57. Petros TJ, Shrestha BR, Mason C (2009) Specificity and sufficiency of EphB1 in driving the ipsilateral retinal projection. J Neurosci 29(11):3463–3474. https://doi.org/10.1523/JNEUROSCI.5655-08.2009
58. Jin K, Xiang M (2012) In vitro explant culture and related protocols for the study of mouse retinal development. Methods Mol Biol 884:155–165. https://doi.org/10.1007/978-1-61779-848-1_10
59. Dick E, Miller RF (1985) Extracellular K+ activity changes related to electroretinogram components. I. Amphibian (I-type) retinas. J Gen Physiol 85(6):885–909
60. Stockton RA, Slaughter MM (1989) B-wave of the electroretinogram. A reflection of ON bipolar cell activity. J Gen Physiol 93(1):101–122
61. Robson JG, Maeda H, Saszik SM, Frishman LJ (2004) In vivo studies of signaling in rod pathways of the mouse using the electroretinogram. Vis Res 44(28):3253–3268. https://doi.org/10.1016/j.visres.2004.09.002
62. Mears AJ, Kondo M, Swain PK, Takada Y, Bush RA, Saunders TL, Sieving PA, Swaroop A (2001) Nrl is required for rod photoreceptor development. Nat Genet 29(4):447–452
63. Furukawa T, Morrow EM, Cepko CL (1997) Crx, a novel otx-like homeobox gene, shows photoreceptor-specific expression and regulates photoreceptor differentiation. Cell 91(4):531–541
64. Chen J, Rattner A, Nathans J (2005) The rod photoreceptor-specific nuclear receptor Nr2e3 represses transcription of multiple cone-specific genes. J Neurosci 25(1):118–129
65. Corbo JC, Cepko CL (2005) A hybrid photoreceptor expressing both rod and cone genes in a mouse model of enhanced S-cone syndrome. PLoS Genet 1(2):e11
66. Peng GH, Ahmad O, Ahmad F, Liu J, Chen S (2005) The photoreceptor-specific nuclear receptor Nr2e3 interacts with Crx and exerts opposing effects on the transcription of rod versus cone genes. Hum Mol Genet 14(6):747–764
67. Misra K, Luo H, Li S, Matise M, Xiang M (2014) Asymmetric activation of Dll4-notch signaling by Foxn4 and proneural factors activates BMP/TGFbeta signaling to specify V2b interneurons in the spinal cord. Development 141(1):187–198. https://doi.org/10.1242/dev.092536
68. Wu F, Li R, Umino Y, Kaczynski TJ, Sapkota D, Li S, Xiang M, Fliesler SJ, Sherry DM, Gannon M, Solessio E, Mu X (2013) Onecut1 is essential for horizontal cell genesis and retinal integrity. J Neurosci 33 (32):13053–13065, 13065a. https://doi.org/10.1523/JNEUROSCI.0116-13.2013
69. Keeley PW, Luna G, Fariss RN, Skyles KA, Madsen NR, Raven MA, Poche RA, Swindell EC et al (2013) Development and plasticity of outer retinal circuitry following genetic removal of horizontal cells. J Neurosci 33(45):17847–17862. https://doi.org/10.1523/JNEUROSCI.1373-13.2013
70. Sonntag S, Dedek K, Dorgau B, Schultz K, Schmidt KF, Cimiotti K, Weiler R, Lowel S et al (2012) Ablation of retinal horizontal cells from adult mice leads to rod degeneration and remodeling in the outer retina. J Neurosci 32(31):10713–10724. https://doi.org/10.1523/JNEUROSCI.0442-12.2012